

# Supplementary Topics

CHAPTER

10

In Chapter 1, we learned the basic mathematical tools and physical concepts of vectors and fields. In Chapters 2 and 3, we learned the fundamental laws of electromagnetics, namely, Maxwell's equations, first in integral form and then in differential form. Then in Chapters 4 through 9, we extended our study to the fundamental electromagnetic concepts and phenomena, as relevant to electrical and computer engineering. These comprised the propagation, transmission, and radiation of electromagnetic waves, as well as the thread of statics-quasistatics-waves to bring out the frequency behavior of physical structures.

This final chapter is devoted to six independent topics, each one based on, and hence supplementary to, one or more of Chapters 4 through 9. The six topics can be studied independently following the respective chapters on which they are based. These supplementary topics, although independent of each other, have the common goal of extending the knowledge gained in the corresponding previous chapter(s) for the purpose of illustrating a concept, phenomenon, or application.

## 10.1 WAVE PROPAGATION IN IONIZED MEDIUM

In Chapter 4, we studied uniform plane wave propagation in free space. In this section, we shall extend the discussion to wave propagation in ionized medium. An example of ionized medium is the earth's ionosphere, which is a region of the upper atmosphere extending from approximately 50 km to more than 1000 km above the earth. In this region, the constituent gases are ionized, mostly because of ultraviolet radiation from the sun, thereby resulting in the production of positive ions and electrons that are free to move under the influence of the fields of a wave incident upon the medium. The positive ions are, however, heavy compared to electrons and hence they are relatively immobile. The electron motion produces a current that influences the wave propagation.

In fact, in Section 1.5 we considered the motion of a cloud of electrons of uniform density  $N$  under the influence of a time-varying electric field

$$\mathbf{E} = E_0 \cos \omega t \mathbf{a}_x \quad (10.1)$$

and found that the resulting current density is given by

$$\mathbf{J} = \frac{Ne^2}{m\omega} E_0 \sin \omega t \mathbf{a}_x = \frac{Ne^2}{m} \int \mathbf{E} dt \quad (10.2)$$

where  $e$  and  $m$  are the electronic charge and mass, respectively. This result is based on the mechanism of continuous acceleration of the electrons by the force due to the applied electric field. In the case of the ionized medium, the electron motion is, however, impeded by the collisions of the electrons with the heavy particles and other electrons. We shall ignore these collisions as well as the negligible influence of the magnetic field associated with the wave.

Considering uniform plane wave propagation in the  $z$ -direction in an unbounded ionized medium, and with the electric field oriented in the  $x$ -direction, we then have

$$\frac{\partial E_x}{\partial z} = -\frac{\partial B_y}{\partial t} = -\mu_0 \frac{\partial H_y}{\partial t} \quad (10.3a)$$

$$\frac{\partial H_y}{\partial z} = -J_x - \frac{\partial D_x}{\partial t} = -\frac{Ne^2}{m} \int E_x dt - \epsilon_0 \frac{\partial E_x}{\partial t} \quad (10.3b)$$

Differentiating (10.3a) with respect to  $z$  and then substituting for  $\partial H_y/\partial z$  from (10.3b), we obtain the wave equation

$$\begin{aligned} \frac{\partial^2 E_x}{\partial z^2} &= -\mu_0 \frac{\partial}{\partial t} \left[ -\frac{Ne^2}{m} \int E_x dt - \epsilon_0 \frac{\partial E_x}{\partial t} \right] \\ &= \frac{\mu_0 Ne^2}{m} E_x + \mu_0 \epsilon_0 \frac{\partial^2 E_x}{\partial t^2} \end{aligned} \quad (10.4)$$

Substituting

$$E_x = E_0 \cos(\omega t - \beta z) \quad (10.5)$$

corresponding to the uniform plane wave solution into (10.4) and simplifying, we get

$$\begin{aligned} \beta^2 &= \omega^2 \mu_0 \epsilon_0 - \frac{\mu_0 Ne^2}{m} \\ &= \omega^2 \mu_0 \epsilon_0 \left( 1 - \frac{Ne^2}{m \epsilon_0 \omega^2} \right) \end{aligned}$$

Thus, the phase constant for propagation in the ionized medium is given by

$$\beta = \omega \sqrt{\mu_0 \epsilon_0 \left( 1 - \frac{Ne^2}{m \epsilon_0 \omega^2} \right)} \quad (10.6)$$

This result indicates that the ionized medium behaves as though the permittivity of free space is modified by the multiplying factor  $[1 - (Ne^2/m\epsilon_0\omega^2)]$ . We may therefore write

$$\beta = \omega\sqrt{\mu_0\epsilon_{\text{eff}}} \quad (10.7)$$

where

$$\epsilon_{\text{eff}} = \epsilon_0\left(1 - \frac{Ne^2}{m\epsilon_0\omega^2}\right) \quad (10.8)$$

is the *effective permittivity* of the ionized medium. We note that for  $\omega \rightarrow \infty$ ,  $\epsilon_{\text{eff}} \rightarrow \epsilon_0$  and the medium behaves just as free space. This is to be expected since (10.2) indicates that for  $\omega \rightarrow \infty$ ,  $\mathbf{J} \rightarrow 0$ . As  $\omega$  decreases from  $\infty$ ,  $\epsilon_{\text{eff}}$  becomes less and less until for  $\omega$  equal to  $\sqrt{Ne^2/m\epsilon_0}$ ,  $\epsilon_{\text{eff}}$  becomes zero. Hence for  $\omega > \sqrt{Ne^2/m\epsilon_0}$ ,  $\epsilon_{\text{eff}}$  is positive,  $\beta$  is real, and the solution for the electric field remains to be that of a propagating wave. For  $\omega < \sqrt{Ne^2/m\epsilon_0}$ ,  $\epsilon_{\text{eff}}$  is negative,  $\beta$  becomes imaginary, and the solution for the electric field corresponds to no propagation.

Thus, waves of frequency  $f > \sqrt{Ne^2/4\pi^2m\epsilon_0}$  propagate in the ionized medium and waves of frequency  $f < \sqrt{Ne^2/4\pi^2m\epsilon_0}$  do not propagate. The quantity  $\sqrt{Ne^2/4\pi^2m\epsilon_0}$  is known as the *plasma frequency* and is denoted by the symbol,  $f_N$ . Substituting values for  $e$ ,  $m$ , and  $\epsilon_0$ , we get

$$f_N = \sqrt{80.6N} \text{ Hz} \quad (10.9)$$

where  $N$  is in electrons per meter cubed. We can now write  $\epsilon_{\text{eff}}$  as

$$\epsilon_{\text{eff}} = \epsilon_0\left(1 - \frac{f_N^2}{f^2}\right) \quad (10.10)$$

Proceeding further, we obtain the phase velocity for the propagating range of frequencies, that is, for  $f > f_N$ , to be

$$\begin{aligned} v_p &= \frac{1}{\sqrt{\mu_0\epsilon_{\text{eff}}}} = \frac{1}{\sqrt{\mu_0\epsilon_0(1 - f_N^2/f^2)}} \\ &= \frac{c}{\sqrt{1 - f_N^2/f^2}} \end{aligned} \quad (10.11)$$

where  $c = 1/\sqrt{\mu_0\epsilon_0}$  is the velocity of light in free space. From (10.11), we observe that  $v_p > c$  and is a function of the wave frequency. The fact that  $v_p > c$  is not a violation of the principle of relativity, since the dispersive nature of the medium resulting from the dependence of  $v_p$  upon  $f$  ensures that information always travels with a velocity less than  $c$ . The topic of *dispersion* is discussed in Section 8.3.

To apply what we have learned above concerning propagation in an ionized medium to the case of the earth's ionosphere, we first provide a brief description of the ionosphere. A typical distribution of the ionospheric electron density versus height above the earth is shown in Figure 10.1. The electron density exists in the form of several layers known as  $D$ ,  $E$ , and  $F$  layers in which the ionization changes with the hour of the day, the

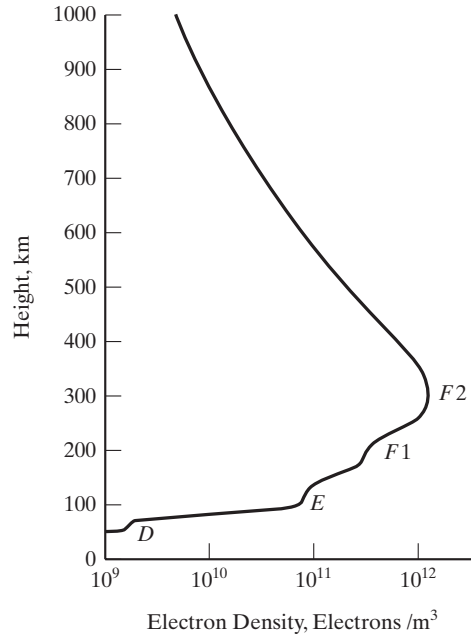


FIGURE 10.1

A typical distribution of ionospheric electron density versus height above the earth.

season, the sunspot cycle, and the geographic location. The nomenclature behind the designation of the letters for the layers is due to Appleton in England, who in 1925 and at about the same time as Breit and Tuve in the United States demonstrated experimentally the reflection of radio waves by the ionosphere. In his early work, Appleton was accustomed to writing *E* for the electric field of the wave reflected from the first layer he recognized. Later, when he recognized a second layer, at a greater height, he wrote *F* for the field of the wave reflected from it. Still later, he conjectured that there might be a third layer lower from either of the first two and thus he decided to name the possible lower layer *D*, thereby leaving earlier letters of the alphabet for other possible undiscovered, still lower layers. Electrons were indeed detected later in the *D* region.

The *D* region extends over the altitude range of about 50 km to about 90 km. Since collisions between electrons and heavy particles cannot be neglected in this region, it is mainly an absorbing region. The *E* region extends from about 90 km to about 150 km. Diurnal and seasonal variations of the *E* layer electron density are strongly correlated with the zenith angle of the sun. In the *F* region, the lower of the two strata is designated as the *F1* layer and the higher, more intense ionized stratum is designated as the *F2* layer. The *F1* ledge is usually located between 160 km and 200 km. Above this region, the *F2* layer electron density increases with altitude, reaching a peak at a height generally lying between 250 km and 400 km. Above this peak the electron density decreases monotonically with altitude. The *F1* ledge is present only during the day. During the night, the *F1* and *F2* layers are identified as a single *F* layer. The *F2* layer is the most important from the point of view of radio communication since it contains the greatest concentration of electrons. Paradoxically, it also exhibits several anomalies.

Wave propagation in the ionosphere is complicated by the presence of the earth's magnetic field. If we neglect the earth's magnetic field, then for a wave of frequency  $f$  incident vertically on the ionosphere from a transmitter on the ground, it is evident from the propagation condition  $f > f_N$  that the wave propagates up to the height at which  $f = f_N$ , and since it cannot propagate beyond that height, it gets reflected at that height. Thus, waves of frequencies less than the maximum plasma frequency corresponding to the peak of the  $F2$  layer cannot penetrate the ionosphere. Hence, for communication with satellites orbiting above the peak of the ionosphere, frequencies greater than this maximum plasma frequency, also known as the *critical frequency*, must be employed. While this critical frequency is a function of the time of day, the season, the sunspot cycle, and the geographic location, it is not greater than about 15 MHz and can be as low as a few megahertz. For a wave incident obliquely on the ionosphere, reflection is possible for frequencies greater than the critical frequency, up to about three times its value. Hence, for earth-to-satellite communication, frequencies generally exceeding about 40 MHz are employed. Lower frequencies permit long-distance, ground-to-ground communication via reflections from the ionospheric layers. This mode of propagation is familiarly known as the *sky wave mode* of propagation. For very low frequencies of the order of several kilohertz and less, the lower boundary of the ionosphere and the earth form a waveguide, thereby permitting waveguide mode of propagation.

In this section, we learned that in an ionized medium, wave propagation occurs only for frequencies exceeding the plasma frequency corresponding to the electron density. Applying this to the case of the earth's ionosphere, we found that this imposes a lower limit in frequency for communication with satellites.

## REVIEW QUESTIONS

- 10.1. What is an ionized medium? What influences wave propagation in an ionized medium?
- 10.2. Provide physical explanation for the frequency dependence of the effective permittivity of an ionized medium.
- 10.3. Discuss the condition for propagation in an ionized medium.
- 10.4. What is plasma frequency? How is it related to the electron density?
- 10.5. Provide a brief description of the earth's ionosphere and discuss how it affects communication.

## PROBLEMS

- 10.1. Show that the units of  $\sqrt{Ne^2/m\epsilon_0}$  is (seconds) $^{-1}$  and that  $e^2/4\pi^2m\epsilon_0$  is equal to 80.6.
- 10.2. Assume the ionosphere to be represented by a parabolic distribution of electron density as given by

$$N(h) = \frac{10^{14}}{80.6} \left[ 1 - \left( \frac{h - 300}{100} \right)^2 \right] \text{ electrons/m}^3 \quad \text{for } 200 < h < 400$$

where  $h$  is the height above the ground in kilometers. (a) Find the height at which a vertically incident wave of frequency 8 MHz is reflected. (b) Find the frequency of a vertically incident wave which gets reflected at a height of 220 km. (c) What is the lowest frequency below which communication is not possible across the peak of the layer?

- 10.3.** For a uniform plane wave of frequency 10 MHz propagating normal to a slab of ionized medium of thickness 50 km and uniform plasma frequency 8 MHz, find (a) the phase velocity in the slab, (b) the wavelength in the slab, and (c) the number of wavelengths undergone by the wave in the slab.

## 10.2 WAVE PROPAGATION IN ANISOTROPIC MEDIUM

In Section 5.1, we learned that for certain dielectric materials known as *anisotropic dielectric materials*,  $\mathbf{D}$  is not in general parallel to  $\mathbf{E}$  and the relationship between  $\mathbf{D}$  and  $\mathbf{E}$  is expressed by means of a permittivity tensor consisting of a  $3 \times 3$  matrix. Similarly, in Section 5.2 we learned of the anisotropic property of certain magnetic materials. There are several important applications based on wave propagation in anisotropic materials. A general treatment is, however, very involved. Hence, we shall consider two simple cases.

For the first example, we consider an anisotropic dielectric medium characterized by the  $\mathbf{D}$  to  $\mathbf{E}$  relationship given by

$$\begin{bmatrix} D_x \\ D_y \\ D_z \end{bmatrix} = \begin{bmatrix} \epsilon_{xx} & 0 & 0 \\ 0 & \epsilon_{yy} & 0 \\ 0 & 0 & \epsilon_{zz} \end{bmatrix} \begin{bmatrix} E_x \\ E_y \\ E_z \end{bmatrix} \quad (10.12)$$

and having the permeability  $\mu_0$ . This simple form of permittivity tensor can be achieved in certain anisotropic liquids and crystals by an appropriate choice of the coordinate system. It is easy to see that the characteristic polarizations for this case are all linear, directed along the coordinate axes and having the effective permittivities  $\epsilon_{xx}$ ,  $\epsilon_{yy}$ , and  $\epsilon_{zz}$  for the  $x$ -,  $y$ -, and  $z$ -directed polarizations, respectively. Let us consider a uniform plane wave propagating in the  $z$ -direction. The wave will generally contain both  $x$ - and  $y$ -components of the fields. It can be decomposed into two waves, one having an  $x$ -directed electric field and the other having a  $y$ -directed electric field. These component waves travel individually in the anisotropic medium as though it is isotropic but with different phase velocities, since the effective permittivities are different. In view of this, the phase relationship between the two waves, and hence the polarization of the composite wave, changes with distance along the direction of propagation.

To illustrate the foregoing discussion quantitatively, let us consider the electric field of the wave to be linearly polarized at  $z = 0$ , as given by

$$\mathbf{E}(0) = (E_{x0} \mathbf{a}_x + E_{y0} \mathbf{a}_y) \cos \omega t \quad (10.13)$$

Then assuming (+) wave only, the electric field at an arbitrary value of  $z$  is given by

$$\mathbf{E}(z) = E_{x0} \cos(\omega t - \beta_1 z) \mathbf{a}_x + E_{y0} \cos(\omega t - \beta_2 z) \mathbf{a}_y \quad (10.14)$$

where

$$\beta_1 = \omega \sqrt{\mu_0 \epsilon_{xx}} \quad (10.15a)$$

$$\beta_2 = \omega \sqrt{\mu_0 \epsilon_{yy}} \quad (10.15b)$$

are the phase constants corresponding to the  $x$ -polarized and  $y$ -polarized component waves, respectively. Thus, the phase difference between the  $x$ - and  $y$ -components of the field is given by

$$\Delta\phi = (\beta_2 - \beta_1)z \quad (10.16)$$

As the composite wave progresses along the  $z$ -direction,  $\Delta\phi$  changes from zero at  $z = 0$  to  $\pi/2$  at  $z = \pi/2(\beta_2 - \beta_1)$  to  $\pi$  at  $z = \pi/(\beta_2 - \beta_1)$ , and so on. The polarization of the composite wave thus changes from linear at  $z = 0$  to elliptical for  $z > 0$ , becoming linear again at  $z = \pi/(\beta_2 - \beta_1)$ , but rotated by an angle of  $2 \tan^{-1}(E_{y0}/E_{x0})$ , as shown in Figure 10.2. Thereafter, it becomes elliptical again, returning back to the original linear polarization at  $z = 2\pi/(\beta_2 - \beta_1)$ , and so on.

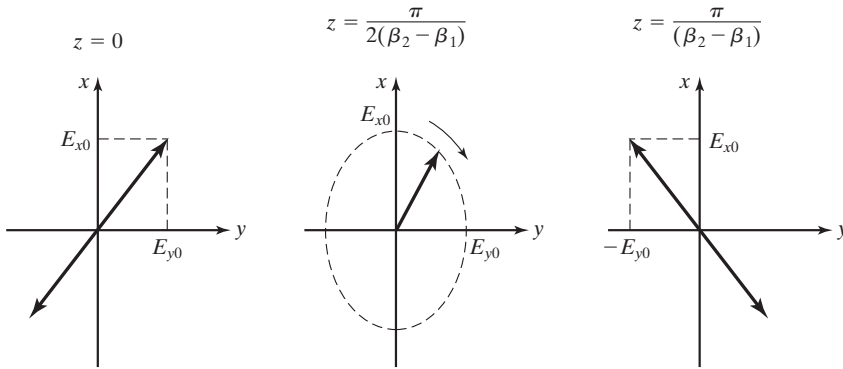


FIGURE 10.2

The change in polarization of the field of a wave propagating in the anisotropic dielectric medium characterized by equation (10.12).

For the second example, we consider propagation in a ferrite medium. Ferrites are a class of magnetic materials which, when subject to a d.c. magnetizing field, exhibit anisotropic magnetic properties. Since there are phase differences associated with the relationships between the components of  $\mathbf{B}$  and the components of  $\mathbf{H}$  due to this anisotropy, it is convenient to use the phasor notation and write the relationship in terms of the phasor components. For an applied d.c. magnetic field along the direction of propagation of the wave, which we assume to be the  $z$ -direction, this relationship is given by

$$\begin{bmatrix} \bar{B}_x \\ \bar{B}_y \\ \bar{B}_z \end{bmatrix} = \begin{bmatrix} \mu & -j\kappa & 0 \\ j\kappa & \mu & 0 \\ 0 & 0 & \mu_0 \end{bmatrix} \begin{bmatrix} \bar{H}_x \\ \bar{H}_y \\ \bar{H}_z \end{bmatrix} \quad (10.17)$$

where  $\mu$  and  $\kappa$  depend upon the material, the strength of the d.c. magnetic field, and the wave frequency.

To find the characteristic polarizations, we first note from (10.17) that

$$\bar{B}_x = \mu\bar{H}_x - j\kappa\bar{H}_y \quad (10.18a)$$

$$\bar{B}_y = j\kappa\bar{H}_x + \mu\bar{H}_y \quad (10.18b)$$

Setting  $\bar{B}_x/\bar{B}_y$  equal to  $\bar{H}_x/\bar{H}_y$ , we then have

$$\frac{\mu\bar{H}_x - j\kappa\bar{H}_y}{j\kappa\bar{H}_x + \mu\bar{H}_y} = \frac{\bar{H}_x}{\bar{H}_y}$$

which upon solution for  $\bar{H}_x/\bar{H}_y$  gives

$$\frac{\bar{H}_x}{\bar{H}_y} = \pm j \quad (10.19)$$

This result corresponds to equal amplitudes of  $H_x$  and  $H_y$  and phase difference of  $\pm 90^\circ$ . Thus, the characteristic polarizations are both circular, rotating in opposite senses as viewed along the  $z$ -direction.

The effective permeabilities of the ferrite medium corresponding to the characteristic polarizations are

$$\begin{aligned} \frac{\bar{B}_x}{\bar{H}_x} &= \frac{\mu\bar{H}_x - j\kappa\bar{H}_y}{\bar{H}_x} \\ &= \mu - j\kappa\frac{\bar{H}_y}{\bar{H}_x} \\ &= \mu \mp \kappa \quad \text{for } \frac{\bar{H}_x}{\bar{H}_y} = \pm j \end{aligned} \quad (10.20)$$

The phase constants associated with the propagation of the characteristic waves are

$$\beta_{\pm} = \omega\sqrt{\epsilon(\mu \mp \kappa)} \quad (10.21)$$

where the subscripts  $+$  and  $-$  refer to  $\bar{H}_x/\bar{H}_y = +j$  and  $\bar{H}_x/\bar{H}_y = -j$ , respectively. We note from (10.21) that  $\beta_+$  can become imaginary if  $(\mu - \kappa) < 0$ . When this happens, wave propagation does not occur for that characteristic polarization. We shall hereafter assume that the wave frequency is such that both characteristic waves propagate.

Let us now consider the magnetic field of the wave to be linearly polarized in the  $x$  direction at  $z = 0$ , that is,

$$\mathbf{H}(0) = H_0 \cos \omega t \mathbf{a}_x \quad (10.22)$$

Then we can express (10.22) as the superposition of two circularly polarized fields having opposite senses of rotation in the  $xy$ -plane in the manner

$$\begin{aligned} \mathbf{H}(0) &= \left( \frac{H_0}{2} \cos \omega t \mathbf{a}_x + \frac{H_0}{2} \sin \omega t \mathbf{a}_y \right) \\ &+ \left( \frac{H_0}{2} \cos \omega t \mathbf{a}_x - \frac{H_0}{2} \sin \omega t \mathbf{a}_y \right) \end{aligned} \quad (10.23)$$

The circularly polarized field inside the first pair of parentheses on the right side of (10.23) corresponds to

$$\frac{\bar{H}_x}{\bar{H}_y} = \frac{H_0/2}{-jH_0/2} = +j$$

whereas that inside the second pair of parentheses corresponds to

$$\frac{\bar{H}_x}{\bar{H}_y} = \frac{H_0/2}{jH_0/2} = -j$$

Assuming propagation in the positive  $z$ -direction, the field at an arbitrary value of  $z$  is then given by

$$\begin{aligned} \mathbf{H}(z) &= \left[ \frac{H_0}{2} \cos(\omega t - \beta_+ z) \mathbf{a}_x + \frac{H_0}{2} \sin(\omega t - \beta_+ z) \mathbf{a}_y \right] \\ &\quad + \left[ \frac{H_0}{2} \cos(\omega t - \beta_- z) \mathbf{a}_x - \frac{H_0}{2} \sin(\omega t - \beta_- z) \mathbf{a}_y \right] \\ &= \left[ \frac{H_0}{2} \cos\left(\omega t - \frac{\beta_+ + \beta_-}{2} z - \frac{\beta_+ - \beta_-}{2} z\right) \mathbf{a}_x \right. \\ &\quad \left. + \frac{H_0}{2} \sin\left(\omega t - \frac{\beta_+ + \beta_-}{2} z - \frac{\beta_+ - \beta_-}{2} z\right) \mathbf{a}_y \right] \\ &\quad + \left[ \frac{H_0}{2} \cos\left(\omega t - \frac{\beta_+ + \beta_-}{2} z + \frac{\beta_+ - \beta_-}{2} z\right) \mathbf{a}_x \right. \\ &\quad \left. - \frac{H_0}{2} \sin\left(\omega t - \frac{\beta_+ + \beta_-}{2} z + \frac{\beta_+ - \beta_-}{2} z\right) \mathbf{a}_y \right] \\ &= \left[ H_0 \cos\left(\frac{\beta_- - \beta_+}{2} z\right) \mathbf{a}_x + H_0 \sin\left(\frac{\beta_- - \beta_+}{2} z\right) \mathbf{a}_y \right] \\ &\quad \cdot \cos\left(\omega t - \frac{\beta_+ + \beta_-}{2} z\right) \end{aligned} \quad (10.24)$$

The result given by (10.24) indicates that the  $x$ - and  $y$ -components of the field are in phase at any given value of  $z$ . Hence, the field is linearly polarized for all values of  $z$ . The direction of polarization is, however, a function of  $z$  since

$$\frac{H_y}{H_x} = \frac{H_0 \sin[(\beta_- - \beta_+)/2]z}{H_0 \cos[(\beta_- - \beta_+)/2]z} = \tan \frac{\beta_- - \beta_+}{2} z \quad (10.25)$$

and hence the angle made by the field vector with the  $x$ -axis is  $[(\beta_- - \beta_+)/2]z$ . Thus, the direction of polarization rotates linearly with  $z$  at a rate of  $(\beta_- - \beta_+)/2$ . This phenomenon is known as *Faraday rotation* and is illustrated with the aid of the sketches in Figure 10.3. The sketches in any given column correspond to a fixed value of  $z$ , whereas the sketches in a given row correspond to a fixed value of  $t$ . At  $z = 0$ , the field

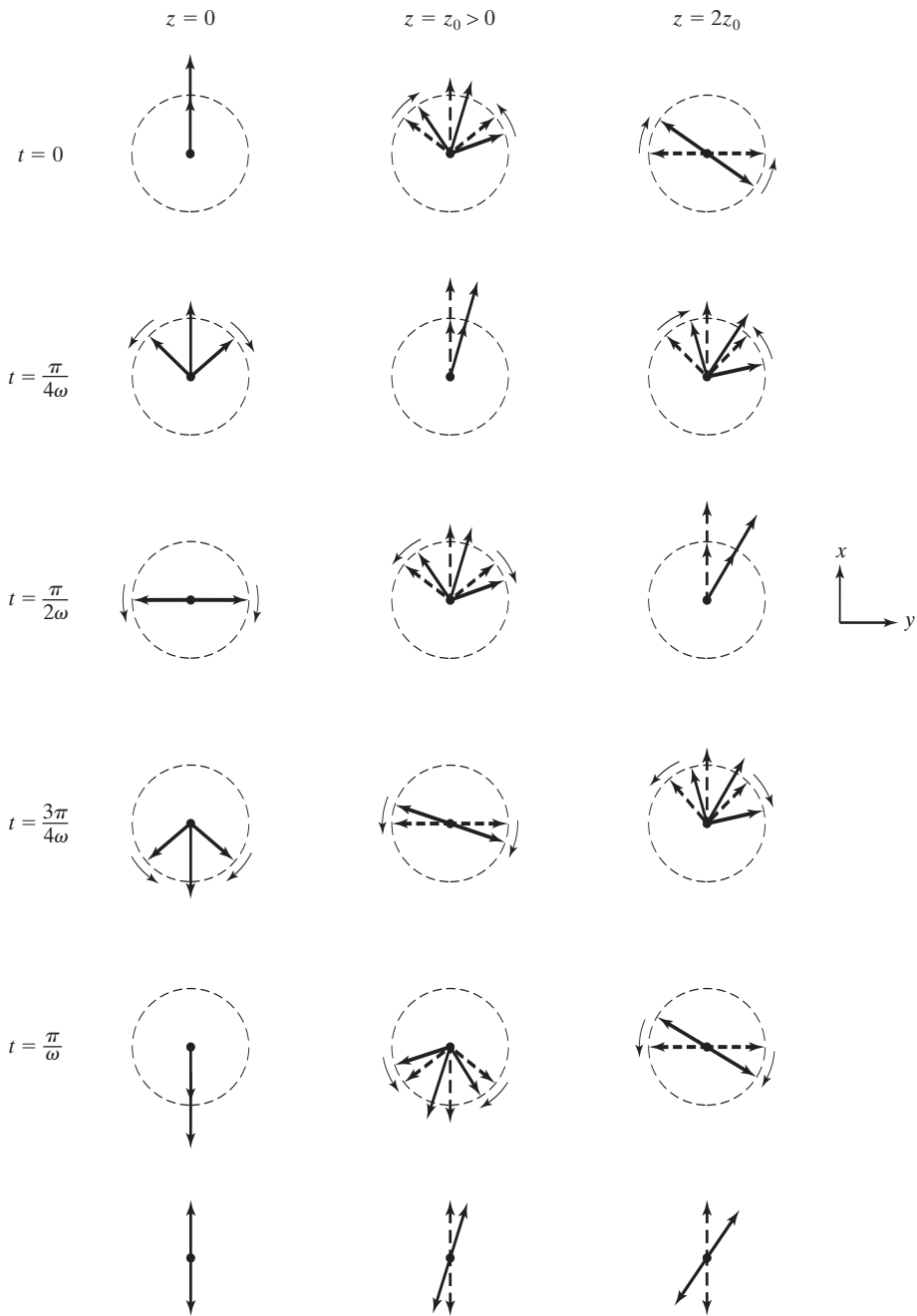
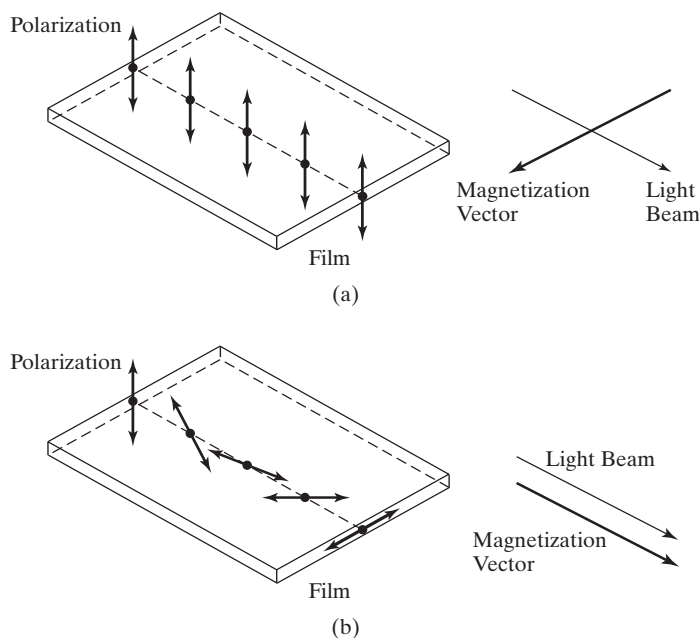


FIGURE 10.3  
For illustrating the phenomenon of Faraday rotation.

is linearly polarized in the  $x$ -direction and is the superposition of two counter-rotating circularly polarized fields, as shown by the time series of sketches in the first column. If the medium is isotropic, the two counter-rotating circularly polarized fields undergo the same amount of phase lag with  $z$  and the field remains linearly polarized in the  $x$ -direction, as shown by the dashed lines in the second and third columns. For the case of the anisotropic medium, the two circularly polarized fields undergo different amounts of phase lag with  $z$ . Hence, their superposition results in a linear polarization making an angle with the  $x$ -direction and increasing linearly with  $z$ , as shown by the solid lines in the second and third columns.

The phenomenon of Faraday rotation in a ferrite medium that we have just discussed forms the basis for a number of devices in the microwave field. The phenomenon itself is not restricted to ferrites. For example, an ionized medium immersed in a d.c. magnetic field possesses anisotropic properties that give rise to Faraday rotation of a linearly polarized wave propagating along the d.c. magnetic field. A natural example of this is propagation along the earth's magnetic field in the ionosphere. A simple modern example of the application of Faraday rotation is, however, illustrated by the magneto-optical switch. In fact, Faraday rotation was originally discovered in the optics regime.

The magneto-optical switch is a device for modulating a laser beam by switching on and off an electric current. The electric current generates a magnetic field that rotates the magnetization vector in a magnetic iron-garnet film on a substrate of garnet, in the plane of the film through which a light wave passes. When it enters the film, the light wave field is linearly polarized normal to the plane of the film. If the current in the electric circuit is off, the magnetization vector is normal to the direction of propagation of the wave and the wave emerges out of the film without change of polarization, as shown in Figure 10.4(a). If the current in the electric circuit is on,



**FIGURE 10.4**  
For illustrating the principle of operation of a magneto-optical switch.

the magnetization vector is parallel to the direction of propagation of the wave, the light wave undergoes Faraday rotation and emerges out of the film with its polarization rotated by  $90^\circ$ , as shown in Figure 10.4(b). After it emerges out of the film, the light beam is passed through a polarizer which has the property of absorbing light of the original polarization but passing through the light of the  $90^\circ$ -rotated polarization. Thus, the beam is made to turn on and off by the switching on and off of the current in the electric circuit. In this manner, any coded message can be made to be carried by the light beam.

In this section, we discussed wave propagation in an anisotropic medium. In particular, we learned that in a ferrite medium, a linearly polarized wave propagating along the direction of an applied d.c. magnetic field undergoes Faraday rotation. We then briefly mentioned other examples of media in which Faraday rotation takes place and finally discussed the operation of the magneto-optical switch, a device employing Faraday rotation for modulating a light beam.

## REVIEW QUESTIONS

- 10.6. Discuss the principle behind wave propagation in an anisotropic medium based on the decomposition of the wave into characteristic waves.
- 10.7. When does a wave propagate in an anisotropic medium without change in polarization?
- 10.8. What is Faraday rotation? When does Faraday rotation take place in an anisotropic medium?
- 10.9. Consult appropriate reference books and list three applications of Faraday rotation.
- 10.10. What is a magneto-optical switch? Discuss its operation.

## PROBLEMS

- 10.4. For the anisotropic medium characterized by the  $\mathbf{D}$  to  $\mathbf{E}$  relationship given by (10.12), assume  $\epsilon_{xx} = 4\epsilon_0$ ,  $\epsilon_{yy} = 9\epsilon_0$ , and  $\epsilon_{zz} = 2\epsilon_0$ , and find the distance in which the phase difference between the  $x$ - and  $y$ -components of a plane wave of frequency  $10^9$  Hz propagating in the  $z$ -direction changes by the amount  $\pi$ .
- 10.5. Show that for plane wave propagation in an anisotropic medium, the angle between  $\mathbf{E}$  and  $\mathbf{H}$  is not in general equal to  $90^\circ$ . For the anisotropic dielectric medium of Problem 10.4, find the angle between  $\mathbf{E}$  and  $\mathbf{H}$  for  $\mathbf{E}$  linearly polarized along the bisector of the angle between the  $x$ - and  $y$ -axes.
- 10.6. For a wave of frequency  $\omega$ , the quantities  $\mu$  and  $\kappa$  in the permeability matrix of (10.17) are given by

$$\mu = \mu_0 \left[ 1 + \frac{\omega_0 \omega_M}{\omega_0^2 - \omega^2} \right]$$

$$\kappa = -\mu_0 \frac{\omega \omega_M}{\omega_0^2 - \omega^2}$$

where  $\omega_0 = \mu_0 |e| H_0 / m$ ,  $\omega_M = \mu_0 |e| M_0 / m$ ,  $H_0$  is the d.c. magnetizing field,  $M_0$  is the magnetic dipole moment per unit volume in the material in the absence of the wave,  $e$  is the charge of an electron, and  $m$  is the mass of an electron. (a) Show that the effective

permeabilities corresponding to the characteristic polarizations are  $\mu_0 \left[ 1 + \frac{\omega_M}{\omega_0 \mp \omega} \right]$  for  $\vec{H}_x/\vec{H}_y = \pm j$ . (b) Compute the Faraday rotation angle in degrees per centimeter along the  $z$ -direction for  $\omega = 10^{10}$  rad/s, if  $\omega_M = 5 \times 10^{10}$  rad/s,  $\omega_0 = 1.5 \times 10^{10}$  rad/s, and  $\epsilon = 9\epsilon_0$ .

- 10.7.** For the quantities defined in Problem 10.6 for the ferrite medium, show that for  $\omega_0 \ll \omega$  and  $\omega_M \ll \omega$ , the Faraday rotation per unit distance along the  $z$ -direction is  $\frac{\omega_M}{2} \sqrt{\mu_0 \epsilon}$ . Compute its value in degrees per centimeter if  $\omega_M = 5 \times 10^{10}$  rad/s and  $\epsilon = 9\epsilon_0$ .

### 10.3 ELECTROMAGNETIC COMPATIBILITY AND SHIELDING

As stated in the preface of the book, electromagnetics is all around us. Every time we turn on a switch for electrical power or for electronic equipment, every time we press a key on our computer keyboard or on our cell phone, or every time we perform a similar action involving an everyday electrical device, electromagnetics comes into play. While these actions are performed for intentional purposes, the resulting electromagnetic energy may cause unintentional interference of a given system on another system or even one part of a given system on another part of the same system. For example, reception of an FM radio signal may be noisy when the radio is located near a computer, due to radiation from the digital circuits of the computer being received as noise by the radio antenna, thereby degrading the performance of the radio. The computer is said to be causing electromagnetic interference (EMI) in the radio. EMI demonstrates the need for designing systems which are compatible with their electromagnetic environment, which comprises the field of electromagnetic compatibility (EMC).

EMC is defined by IEC (International Electrotechnical Commission) as “the ability of a device, unit of equipment, or system to function satisfactorily in its electromagnetic environment without introducing intolerable electromagnetic disturbances to anything in that environment.” An electromagnetic disturbance may be electromagnetic noise, an unwanted signal, or a change in the propagation medium itself. A system is said to be electromagnetically compatible if (1) it does not cause interference with other systems, (2) it is not susceptible to emission from other systems, and (3) it does not cause interference with itself.

In the analysis and design of systems for EMC work, quasistatic concepts are employed wherever they are applicable, because of simplicity compared to working with complete field solutions. We have learned in Chapter 6 that quasistatic approximations apply when the physical dimensions of the system are much smaller than the wavelength corresponding to the frequency of operation. Thus, three regimes come into play, as follows:

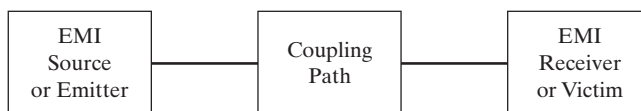
1. When the system is electrically small in all three of its dimensions, that is, when the physical size of the system is such that all three of its dimensions are smaller than the wavelength corresponding to the frequency of operation, then quasistatic approximations hold in all three dimensions and the system can be represented by a lumped circuit equivalent and circuit analysis techniques can be employed.

2. When the physical size of the system is smaller than the wavelength in two of its dimensions and comparable to or larger than the wavelength in the third dimension, then the system becomes a transmission line extending along the longer dimension.
3. When the physical size of the system is such that all three of its dimensions are comparable to or larger than the wavelength, then the analysis entails full field basis using the complete set of Maxwell's equations.

In general, a signal is composed of a spectrum of frequencies. The wavelength above is then the shortest significant wavelength, that is, the wavelength corresponding to the highest frequency of importance in the frequency spectrum of the signal.

As shown in Figure 10.5, all EMC problems can be divided into three parts: (a) source of emission or emitter, (b) receiver of emission or victim, and (c) coupling path or mechanism by means of which emission from the source is transferred to the receiver. In the example of noise in the FM radio due to computer, the source of noise is the computer, the victim is the radio, and the coupling mechanism is the medium between the digital circuits in the computer and the antenna of the radio.

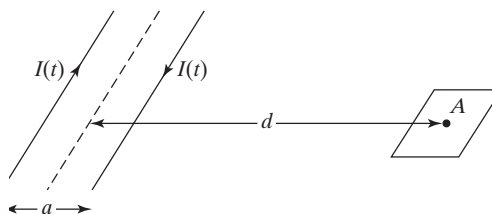
FIGURE 10.5  
The three parts of an EMC problem.



EMC problems can be solved by reducing or eliminating EMI, using one or more of the following three methods: (1) decreasing the emission from the source producing the EMI, (2) making the victim of EMI less susceptible, and (3) making the coupling path less efficient. Although often the only option available to solve an EMC problem is the third one, we shall first consider a simple example of the application of the first two methods.

Thus, let us consider a parallel-wire line consisting of a pair of long, parallel wires of spacing  $a$  and carrying currents  $I(t)$  in opposite directions in the  $z = 0$  plane, as shown in Figure 10.6. Let a small metallic loop of area  $A$  be located in the plane of the loop (the  $xy$ -plane) and such that the distance between the center of the wires to the center of the loop is  $d \gg a$ . The currents in the parallel wires produce a magnetic field, resulting in a time-varying magnetic flux enclosed by the loop and hence voltage induced in the loop, in accordance with Faraday's law, causing EMI in the loop. The EMC problem is to find ways to minimize the EMI in the loop.

FIGURE 10.6  
Arrangement of a metallic loop in the field of a parallel-wire line for illustrating the EMC problem.



The magnetic field due to the parallel wires can be computed from the fact that in the plane transverse to the wires, the fields have the same spatial character as for the static fields corresponding to the same geometry. Thus, applying the result for the magnetic field due to a long wire in Example 2.9 to the two wires and introducing the time variation, we can write the magnetic flux density due to the parallel wires at the center point of the loop to be

$$\mathbf{B} \text{ at center of loop} = \frac{\mu_0 I(t)}{2\pi} \left[ \frac{1}{(d - a/2)} - \frac{1}{(d + a/2)} \right] \quad (10.26a)$$

and directed normal to the area of the loop. For  $d \gg a$ ,

$$\mathbf{B} \text{ at center of loop} \approx \frac{\mu_0 a I(t)}{2\pi d^2} \quad (10.26b)$$

Since the area of the loop is very small compared to its distance from the line, we can assume that the magnetic field does not vary significantly within the area. Assuming also that the current in the wires and hence the magnetic field due to it does not vary significantly in the  $z$ -direction, we obtain the magnetic flux enclosed by the loop to be

$$\psi = \frac{\mu_0 a A I(t)}{2\pi d^2} \quad (10.27)$$

The voltage induced in the loop is then given by

$$V = -\frac{d\psi}{dt} = -\frac{\mu_0 a A}{2\pi d^2} \frac{dI(t)}{dt} \quad (10.28)$$

For  $I(t) = I_0 \cos \omega t$ ,

$$V = \frac{\mu_0 a A I_0 \omega}{2\pi d^2} \sin \omega t \quad (10.29)$$

It can be seen from (10.29) that for the induced voltage to be small,  $I_0$ ,  $a$ ,  $A$ , and  $\omega$  must be as small as possible, and  $d$  should be as large as possible. In a practical situation, some of these parameters may be fixed and only the others may be varied. If the size of the loop cannot be varied, the effective area of the loop can be made smaller by rotating it to make an angle with the plane of the wires. When the angle is  $90^\circ$ , the magnetic field is parallel to the area of the loop and the induced voltage is zero, eliminating the EMC problem. If the spacing between the wires can be varied, another way to decrease EMI is to decrease the spacing, and if possible, for the wires to be twisted. An important observation from (10.29) is that the induced voltage in the loop and hence the EMI increases with frequency. This means that for a nonsinusoidal source, the interference from its frequency components is amplified proportional to the frequency.

As stated earlier, often the only option available to solve an EMC problem is to make the coupling path less efficient. Therefore, it is important to understand the coupling mechanisms. Depending on the separation distance between the source and the victim, different techniques of analysis are used. For small separation distances, circuit models can be used by representing the electric field coupling as *capacitive coupling* and magnetic field coupling as *inductive coupling*. An example of analysis involving capacitive and inductive couplings is considered in Section 10.4, devoted to *crossstalk* on transmission lines, which is interference due to a wave propagating along one transmission line inducing a wave on a neighboring second transmission line. When the source and victim share a common conductor, interference occurs through the common impedance of the conductor, and hence the coupling is termed *common impedance coupling*. The analysis is performed using circuit techniques. For large separation distances between the source and the victim, involving an intervening medium, field techniques are employed involving radiation from the source into the medium and the transfer of the radiated energy from the medium into the victim.

The techniques for the solution of EMC problems, that is, for decreasing the impact of EMI on the victim by making the coupling path less efficient, fall into four categories: (a) proper layout of components and cables, (b) system grounding and bonding, (c) surge suppression and filtering, and (d) shielding. The scope of each of these techniques is extensive by itself. We shall here consider only the topic of shielding by providing an example that makes use of the knowledge from Chapters 5 and 7. Specifically, we shall consider the problem of a plane metallic sheet as a shield for an incident plane wave from a distant source.

The geometry pertaining to the problem is shown in Figure 10.7, in which media 1 and 3 are free space, and medium 2 is a metallic sheet of thickness  $d$ . A uniform plane wave of radian frequency  $\omega$  is incident normally on to the metallic sheet from medium 1. Thus, media 1 and 3 are characterized by the propagation parameters

$$\bar{\gamma}_1 = \bar{\gamma}_3 = j\beta_0 = j\omega/c \tag{10.30a}$$

$$\bar{\eta}_1 = \bar{\eta}_3 = \eta_0 = 120\pi \tag{10.30b}$$

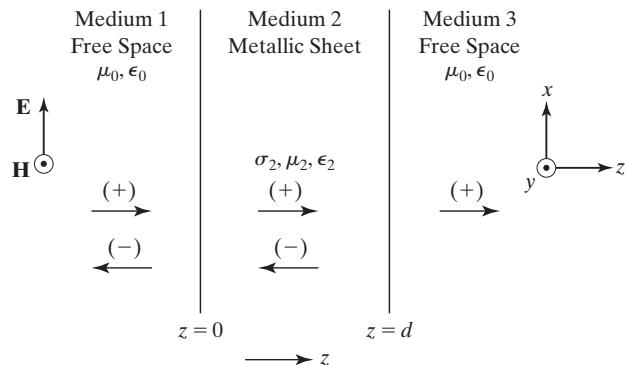


FIGURE 10.7  
Geometry of the arrangement for the analysis of shielding by a metallic sheet.

and medium 2 is characterized by the propagation parameters

$$\bar{\gamma}_2 = \sqrt{j\omega\mu_2(\sigma_2 + j\omega\epsilon_2)} \quad (10.31a)$$

$$\bar{\eta}_2 = \sqrt{\frac{j\omega\mu_2}{\sigma_2 + j\omega\epsilon_2}} \quad (10.31b)$$

It is desired to analyze the system for the shielding effectiveness between medium 1 and medium 3. The *shielding effectiveness* or the *shielding factor*, denoted  $S$ , is defined to be the ratio of the amplitude of the incident electric field in medium 1 to the amplitude of the transmitted electric field in medium 3.

The incident plane wave sets up a reflected wave and a transmitted wave at the interface  $z = 0$ , with the reflected wave propagating back in the negative  $z$ -direction in medium 1 and the transmitted wave propagating in the positive  $z$ -direction in medium 2. When the transmitted wave in medium 2 reaches the interface  $z = d$ , it sets up a reflected wave which propagates back towards the interface  $z = 0$ , and a transmitted wave into medium 3. The reflected wave, when it reaches the interface  $z = 0$ , sets up its own reflection that adds up to the previous transmitted wave due to the incident wave from medium 1. It also sets up a transmitted wave into medium 1, which propagates in the negative  $z$ -direction. The transmitted waves into media 3 and 1 will not set up any reflections, because these media are assumed to extend to infinity in the positive  $z$ - and negative  $z$ -directions, respectively. But each wave in medium 2 sets up a reflected wave and a transmitted wave at the interface on which it is incident. In the steady state, all these transient waves add up and the situation is equivalent to a single (+) wave and a single (-) wave in medium 1, a single (+) wave and a single (-) wave in medium 2, and a single (+) wave in medium 3. Therefore, the complex electric and magnetic field components of the waves in the three media can be written as follows:

Medium 1:

$$\bar{E}_{x1} = \bar{A}_1 e^{-j\beta_0 z} + \bar{B}_1 e^{j\beta_0 z} \quad (10.32a)$$

$$\bar{H}_{y1} = \frac{1}{\eta_0} (\bar{A}_1 e^{-j\beta_0 z} - \bar{B}_1 e^{j\beta_0 z}) \quad (10.32b)$$

Medium 2:

$$\bar{E}_{x2} = \bar{A}_2 e^{-\bar{\gamma}_2 z} + \bar{B}_2 e^{\bar{\gamma}_2 z} \quad (10.33a)$$

$$\bar{H}_{y2} = \frac{1}{\bar{\eta}_2} (\bar{A}_2 e^{-\bar{\gamma}_2 z} - \bar{B}_2 e^{\bar{\gamma}_2 z}) \quad (10.33b)$$

Medium 3:

$$\bar{E}_{x3} = \bar{A}_3 e^{-j\beta_0 z} \quad (10.34a)$$

$$\bar{H}_{y3} = \frac{1}{\eta_0} \bar{A}_3 e^{-j\beta_0 z} \quad (10.34b)$$

According to the definition, the shielding factor,  $S$ , is then equal to  $|\bar{A}_1|/|\bar{A}_3|$ . To find this quantity, we note that the constants  $\bar{A}_1$ ,  $\bar{A}_2$ ,  $\bar{A}_3$ ,  $\bar{B}_1$ , and  $\bar{B}_2$  are related through the boundary conditions at the interfaces  $z = 0$  and  $z = d$ . These are given by

$$\bar{E}_{x1} = \bar{E}_{x2} \quad \text{and} \quad \bar{H}_{y1} = \bar{H}_{y2} \quad \text{at } z = 0 \quad (10.35a)$$

$$\bar{E}_{x2} = \bar{E}_{x3} \quad \text{and} \quad \bar{H}_{y2} = \bar{H}_{y3} \quad \text{at } z = d \quad (10.35b)$$

Thus, we have

$$\bar{A}_1 + \bar{B}_1 = \bar{A}_2 + \bar{B}_2 \quad (10.36a)$$

$$\frac{1}{\eta_0}(\bar{A}_1 - \bar{B}_1) = \frac{1}{\bar{\eta}_2}(\bar{A}_2 - \bar{B}_2) \quad (10.36b)$$

$$\bar{A}_2 e^{-\bar{\gamma}_2 d} + \bar{B}_2 e^{\bar{\gamma}_2 d} = \bar{A}_3 e^{-j\beta_0 d} \quad (10.36c)$$

$$\frac{1}{\bar{\eta}_2}(\bar{A}_2 e^{-\bar{\gamma}_2 d} - \bar{B}_2 e^{\bar{\gamma}_2 d}) = \frac{1}{\eta_0} \bar{A}_3 e^{-j\beta_0 d} \quad (10.36d)$$

Solving (10.36c) and (10.36d) for  $\bar{A}_2$  and  $\bar{B}_2$  in terms of  $\bar{A}_3$ , we obtain

$$\bar{A}_2 = \bar{A}_3 \frac{1}{1 + \bar{\Gamma}_{23}} e^{-j\beta_0 d} e^{\bar{\gamma}_2 d} \quad (10.37a)$$

$$\bar{B}_2 = \bar{A}_2 \bar{\Gamma}_{23} e^{-2\bar{\gamma}_2 d} \quad (10.37b)$$

where

$$\bar{\Gamma}_{23} = \frac{\eta_0 - \bar{\eta}_2}{\eta_0 + \bar{\eta}_2} \quad (10.38)$$

is the electric field reflection coefficient, analogous to the voltage reflection coefficient in transmission-line analysis, for a single transient (+) wave incident from medium 2 onto the interface  $z = d$ . Substituting for  $\bar{B}_2$  in (10.36a) and (10.36b) from (10.37b) and solving for  $\bar{A}_1$  in terms of  $\bar{A}_2$ , we get

$$\bar{A}_1 = \bar{A}_2 \frac{1 + \bar{\Gamma}_{12} \bar{\Gamma}_{23} e^{-2\bar{\gamma}_2 d}}{1 + \bar{\Gamma}_{12}} \quad (10.39)$$

where

$$\bar{\Gamma}_{12} = \frac{\bar{\eta}_2 - \eta_0}{\bar{\eta}_2 + \eta_0} \quad (10.40)$$

is the electric field reflection coefficient for a single transient (+) wave incident from medium 1 onto the interface  $z = 0$ . Note that  $\bar{\Gamma}_{12} = -\bar{\Gamma}_{23}$ . From (10.39) and (10.37a), we then have

$$\frac{\bar{A}_1}{\bar{A}_3} = \frac{1 + \bar{\Gamma}_{12} \bar{\Gamma}_{23} e^{-2\bar{\gamma}_2 d}}{(1 + \bar{\Gamma}_{12})(1 + \bar{\Gamma}_{23})} e^{-j\beta_0 d} e^{\bar{\gamma}_2 d} \quad (10.41)$$

and the shielding factor is given by

$$S = \frac{|\bar{A}_1|}{|\bar{A}_3|} = \frac{|1 + \bar{\Gamma}_{12}\bar{\Gamma}_{23}e^{-2\gamma_2 d}|e^{\alpha_2 d}}{|1 + \bar{\Gamma}_{12}||1 + \bar{\Gamma}_{23}|} \quad (10.42)$$

It can be shown (see Problem 10.8) that this result is also obtainable by formulating the solution in terms of the individual transient waves resulting from bouncing back and forth between the interfaces  $z = d$  and  $z = 0$ , writing field expressions for the individual transient waves and adding them up. Three contributions to the right side of (10.42) can then be identified as follows:

$$\begin{aligned} e^{\alpha_2 d} & \text{— contribution from attenuation in the} \\ & \text{metallic sheet (A)} \\ \left( \frac{1}{|1 + \bar{\Gamma}_{12}||1 + \bar{\Gamma}_{23}|} \right) & \text{— contribution due to transmission from} \\ & \text{free space to the metallic sheet and from} \\ & \text{the metallic sheet to free space (T)} \\ (1 + \bar{\Gamma}_{12}\bar{\Gamma}_{23}e^{-2\bar{\gamma}_2 d}) & \text{— contribution from multiple reflections} \\ & \text{within the metallic sheet (M)} \end{aligned}$$

The general formula for  $S$  given by (10.42) can be simplified for good conductor range of frequencies ( $\sigma_2 \gg \omega\epsilon_2$ ) for the metallic sheet, by recalling from Section 5.4 that for good conductors,

$$\bar{\eta}_2 \approx (1 + j)\sqrt{\pi f \mu_2 / \sigma_2} \quad (10.43)$$

and  $|\bar{\eta}_2| \ll \eta_0$ , so that  $\bar{\Gamma}_{12} \approx -1$ ,  $\bar{\Gamma}_{23} \approx 1$ ,  $(1 + \bar{\Gamma}_{12}) \approx 2\bar{\eta}_2/\eta_0$ , and  $(1 + \bar{\Gamma}_{23}) \approx 2$ . Also, for good conductors,  $\alpha_2 = \beta_2 \approx \sqrt{\pi f \mu_2 \sigma_2}$ . Thus,

$$S \approx \frac{\eta_0}{4|\bar{\eta}_2|} |1 - e^{-2\alpha_2 d} e^{-j2\alpha_2 d}| e^{\alpha_2 d} \quad (10.44)$$

In terms of skin depth  $\delta = 1/\alpha = 1/\sqrt{\pi f \mu_2 \sigma_2}$ , the distance in which the fields are attenuated in the good conductor by the factor  $e^{-1}$ ,

$$S \approx \frac{\eta_0}{4|\bar{\eta}_2|} |1 - e^{-2d/\delta} e^{-j2d/\delta}| e^{d/\delta} \quad (10.45)$$

In terms of decibels,

$$\begin{aligned} S \text{ in dB} &= 20 \log_{10} (\eta_0/4|\bar{\eta}_2|) \\ &+ 20 \log_{10} |1 - e^{-2d/\delta} e^{-j2d/\delta}| \\ &+ 20 \log_{10} e^{d/\delta} \end{aligned} \quad (10.46)$$

with the three terms on the right side identifying the three contributions,  $T$ ,  $M$ , and  $A$ , respectively.

For a numerical example, for copper sheet,  $\sigma_2 = 5.80 \times 10^7$  S/m,  $\mu_2 = \mu_0$ ,  $\epsilon_2 = \epsilon_0$ ,  $\delta = 0.066/\sqrt{f}$  m, and  $|\bar{\eta}_2| = 3.69 \times 10^{-7}\sqrt{f}$   $\Omega$ . For a given set of values of  $d$  and  $f$ , the quantities  $T$ ,  $M$ , and  $A$ , and hence  $S$  can be computed. Table 10.1 shows these quantities for four pairs of values of  $d$  and  $f$ .

TABLE 10.1 Values of  $T$ ,  $M$ ,  $A$ , and  $S$ , for Several Pairs of Values of  $d$  and  $f$  for the Shielding Arrangement of Figure 10.7

$d$ (mm)	$f$ (MHz)	$\delta$ (mm)	$ \bar{\eta}_2 $ ( $\Omega$ )	$d/\delta$	$T$ (db)	$M$ (db)	$A$ (db)	$S$ (db)
1	1	0.066	$3.69 \times 10^{-4}$	15.15	108.14	$\sim 0$	131.59	239.73
1	0.1	0.209	$1.167 \times 10^{-4}$	4.785	118.14	$\sim 0$	41.56	159.70
0.001	1	0.066	$3.69 \times 10^{-4}$	0.015	108.14	-27.59	0.13	80.68
0.001	0.1	0.209	$1.167 \times 10^{-4}$	0.0048	118.14	-37.27	0.042	80.91

From Table 10.1, we can make the following observations:

1. For thick sheets,  $M$  is approximately zero and hence not important.
2. For thin sheets,  $A$  is negligible and  $M$  is important. Furthermore, since  $M$  is negative, meaning that the field is enhanced instead of getting attenuated, it acts counter to the shielding requirement.
3. For thin sheets, increase in  $T$  with decrease in frequency is countered by the increase in magnitude of  $M$ .
4.  $T$  is independent of thickness.

In this section, we introduced the topic of electromagnetic compatibility (EMC), having to do with the design of electrical systems which are compatible with the electromagnetic environment. We learned that the EMC problem can be divided into three parts, (a) source, (b) receiver, and (c) coupling path, and that it can be solved by three methods: (a) decreasing emission from the source, (b) making the receiver less susceptible, and (c) making the coupling path less efficient, which is often the only available option. We provided a simple example of the application of the first two methods. While there are several categories pertinent to the third method, we provided the example of electromagnetic shielding by considering the problem of a plane metallic sheet as a shield for an incident plane wave from a distant source.

## REVIEW QUESTIONS

- 10.11. Describe EMI and EMC. What is IEEE's definition of EMC?
- 10.12. Outline the three regimes that come into play in the design of systems for EMC work.
- 10.13. Specify and discuss the three parts of an EMC problem.
- 10.14. Discuss the example of EMI in a metallic loop located in the field of a parallel-wire line and ways to minimize the EMI.
- 10.15. Outline the solution of the problem of a plane metallic sheet as a shield for an incident plane wave from a distant source.
- 10.16. What is *shielding factor*? Discuss the three contributions to the shielding factor for the plane metallic sheet arrangement.

## PROBLEMS

- 10.8.** For the arrangement of Figure 10.7, obtain the expression for the shielding factor by formulating the solution in terms of the individual transient waves bouncing back and forth between the interfaces  $z = d$  and  $z = 0$ , writing the field expressions for the individual transient waves, and adding them up.
- 10.9.** Compute the value of the shielding factor for a copper shield of thickness 0.01 mm at a frequency of 1 MHz.
- 10.10.** Compute the value of the shielding factor for a steel shield of thickness 0.01 mm at a frequency of 10 MHz. Values of material parameters are as follows:  $\sigma = 5.80 \times 10^6$  S/m,  $\mu = 500\mu_0$ , and  $\epsilon = \epsilon_0$ .

## 10.4 CROSSTALK ON TRANSMISSION LINES

When two or more transmission lines are in the vicinity of one another, a wave propagating along one line, which we shall call the primary line, can induce a wave on another line, the secondary line, due to capacitive (electric field) and inductive (magnetic field) coupling between the two lines, resulting in the undesirable phenomenon of crosstalk between the lines. An example is illustrated by the arrangement of Figure 10.8(a), which is a printed-circuit board (PCB) representation of two closely spaced transmission lines. Figure 10.8(b) represents the distributed circuit equivalent, where  $\mathcal{C}_m$  and  $\mathcal{L}_m$  are the coupling capacitance and coupling inductance, respectively, per unit length of the arrangement.

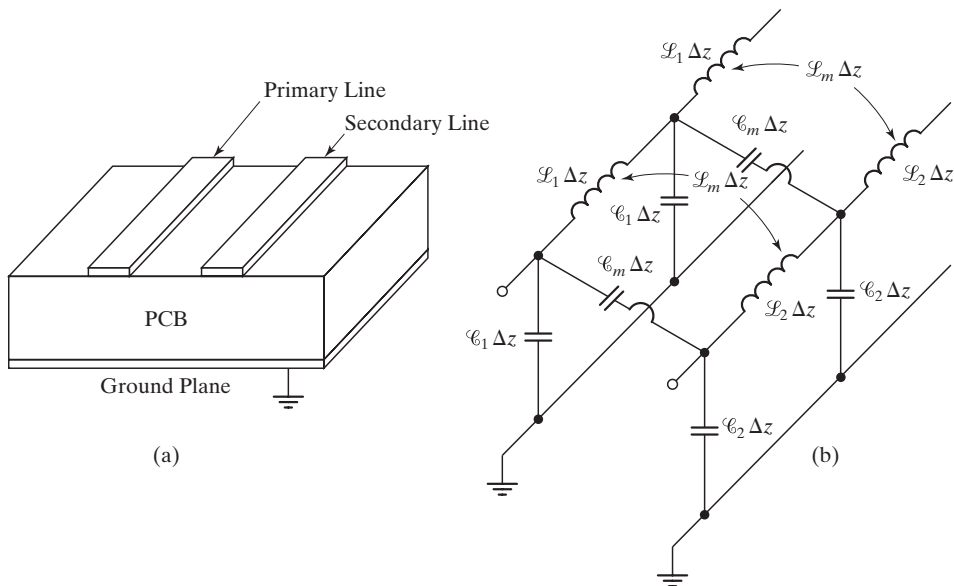


FIGURE 10.8

(a) PCB representation of two closely spaced transmission lines. (b) Distributed equivalent circuit for (a).

In this section, we shall analyze a pair of coupled transmission lines for the determination of induced waves on the secondary line for a given wave on the primary line. To keep the analysis simple, we shall consider both lines to be of the same characteristic impedance, velocity of propagation, and length, and terminated by their characteristic impedances, so that no reflections occur from the ends of either line. It is also convenient to assume the coupling to be weak, so that the effects on the primary line of waves induced in the secondary line can be neglected. Thus, we shall be concerned only with the crosstalk from the primary line to the secondary line and not vice versa. Briefly, as the (+) wave propagates on the primary line from source toward load, each infinitesimal length of that line induces voltage and current in the adjacent infinitesimal length of the secondary line, which set up (+) and (−) waves on that line. The contributions due to the infinitesimal lengths add up to give the induced voltage and current at a given location on the secondary line.

We shall represent the coupled-line pair, as shown in Figure 10.9, with the primary line as line 1 and the secondary line as line 2. Then, when the switch  $S$  is closed at  $t = 0$ , a (+) wave originates at  $z = 0$  on line 1 and propagates toward the load. Let us consider a differential length  $d\xi$  at the location  $z = \xi$  of line 1 charged to the (+) wave voltage and current and obtain its contributions to the induced voltages and currents in line 2.

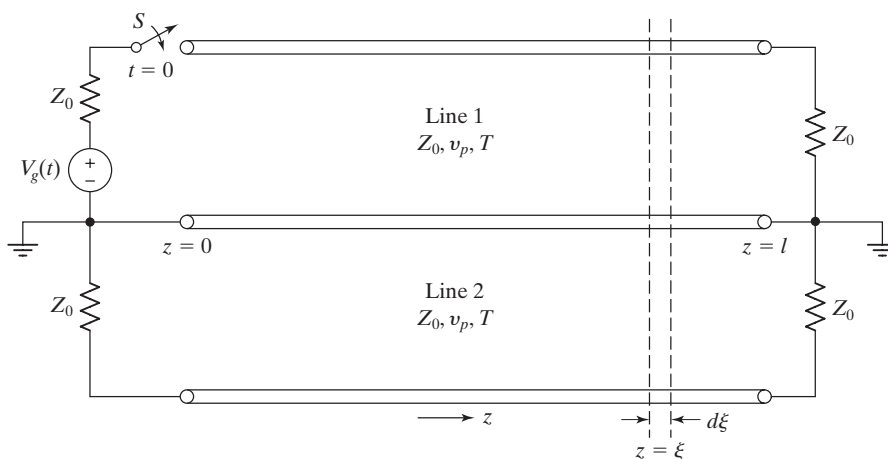


FIGURE 10.9

Coupled transmission-line pair for analysis of crosstalk.

The capacitive coupling induces a differential crosstalk current  $\Delta I_{c2}$ , flowing into the nongrounded conductor of line 2, given by

$$\Delta I_{c2}(\xi, t) = \mathcal{C}_m \Delta \xi \frac{\partial V_1(\xi, t)}{\partial t} \quad (10.47a)$$

where  $V_1(\xi, t)$  is the line-1 voltage. This induced current is modeled by an ideal current source, connected in parallel with line 2 at  $z = \xi$  on that line, as shown in Figure 10.10(a). The current source views the characteristic impedance of the line to either side of  $z = \xi$ ,

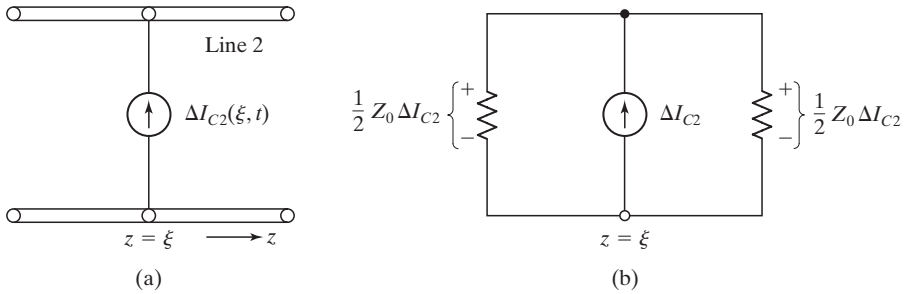


FIGURE 10.10

(a) Modeling for capacitive coupling in crosstalk analysis. (b) Equivalent circuit for (a).

so that the equivalent circuit is as shown in Figure 10.10(b). Thus, voltages of  $\frac{1}{2}Z_0 \Delta I_{C2}$  are produced to the right and left of  $z = \xi$  and propagate as forward-crosstalk and backward-crosstalk voltages, respectively, on line 2.

The inductive coupling induces a differential crosstalk voltage,  $\Delta V_{C2}$ , which is given by

$$\Delta V_{C2}(\xi, t) = \mathcal{L}_m \Delta \xi \frac{\partial I_1(\xi, t)}{\partial t} \quad (10.47b)$$

This induced voltage is modeled by an ideal voltage source in series with line 2 at  $z = \xi$  on that line, as shown in Figure 10.11(a). The polarity of the voltage source is such that the current due to it in line 2 produces a magnetic flux, which opposes the change in the flux due to the current in line 1, in accordance with Lenz's law. The voltage source views the characteristic impedance of the line to either side of it, so that the equivalent circuit is as shown in Figure 10.11(b). Thus, voltages of  $\frac{1}{2}\Delta V_{C2}$  and  $-\frac{1}{2}\Delta V_{C2}$  are produced to the left and right of  $z = \xi$ , respectively, and propagate as backward-crosstalk and forward-crosstalk voltages, respectively, on line 2.

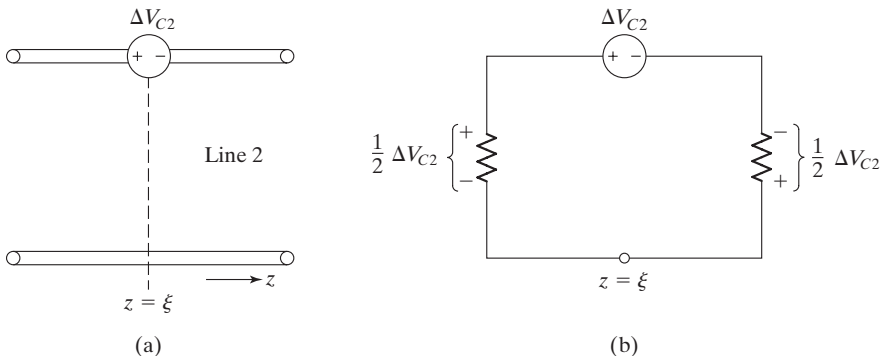


FIGURE 10.11

(a) Modeling for inductive coupling in crosstalk analysis. (b) Equivalent circuit for (a).

Combining the contributions due to capacitive coupling and inductive coupling, we obtain the total differential voltages produced to the right and left of  $z = \xi$  to be

$$\Delta V_2^+ = \frac{1}{2} Z_0 \Delta I_{c2} - \frac{1}{2} \Delta V_{c2} \quad (10.48a)$$

$$\Delta V_2^- = \frac{1}{2} Z_0 \Delta I_{c2} + \frac{1}{2} \Delta V_{c2} \quad (10.48b)$$

respectively. Substituting (10.47a) and (10.47b) into (10.48a) and (10.48b), we obtain

$$\begin{aligned} \Delta V_2^+(\xi, t) &= \left[ \frac{1}{2} \mathcal{C}_m Z_0 \frac{\partial V_1(\xi, t)}{\partial t} - \frac{1}{2} \mathcal{L}_m \frac{\partial I_1(\xi, t)}{\partial t} \right] \Delta \xi \\ &= \frac{1}{2} \left( \mathcal{C}_m Z_0 - \frac{\mathcal{L}_m}{Z_0} \right) \frac{\partial V_1(\xi, t)}{\partial t} \Delta \xi \end{aligned} \quad (10.49a)$$

$$\Delta V_2^-(\xi, t) = \frac{1}{2} \left( \mathcal{C}_m Z_0 + \frac{\mathcal{L}_m}{Z_0} \right) \frac{\partial V_1(\xi, t)}{\partial t} \Delta \xi \quad (10.49b)$$

where we have substituted  $I_1 = V_1/Z_0$ , in accordance with the relationship between the voltage and current of a (+) wave.

We are now ready to apply (10.49a) and (10.49b) in conjunction with superposition to obtain the (+) and (-) wave voltages at any location on line 2, due to a (+) wave of voltage  $V_1(t - z/v_p)$  on line 1. Thus, noting that the effect of  $V_1$  at  $z = \xi$  at a given time  $t$  is felt at a location  $z > \xi$  on line 2 at time  $t + (z - \xi)/v_p$ , we can write

$$\begin{aligned} V_2^+(z, t) &= \int_0^z \frac{1}{2} \left( \mathcal{C}_m Z_0 - \frac{\mathcal{L}_m}{Z_0} \right) \frac{\partial}{\partial t} \left[ V_1 \left( t - \frac{\xi}{v_p} - \frac{z - \xi}{v_p} \right) \right] d\xi \\ &= \frac{1}{2} \left( \mathcal{C}_m Z_0 - \frac{\mathcal{L}_m}{Z_0} \right) \int_0^z \frac{\partial V_1(t - z/v_p)}{\partial t} d\xi \end{aligned} \quad (10.50)$$

or

$$V_2^+(z, t) = z K_f V_1'(t - z/v_p) \quad (10.51)$$

where we have defined

$$K_f = \frac{1}{2} \left( \mathcal{C}_m Z_0 - \frac{\mathcal{L}_m}{Z_0} \right) \quad (10.52)$$

and the prime associated with  $V_1$  denotes differentiation with time. The quantity  $K_f$  is called the *forward-crosstalk coefficient*. Note that the upper limit in the integral in (10.50) is  $z$ , because the line-1 voltage to the right of a given location  $z$  on that line does not contribute to the forward-crosstalk voltage on line 2 at that same location. The result given by (10.51) tells us that the forward-crosstalk voltage is proportional to  $z$  and the time derivative of the primary line voltage.

To obtain  $V_2^-(z, t)$ , we note that the effect of  $V_1$  at  $z = \xi$  at a given time  $t$  is felt at a location  $z < \xi$  on line 2 at time  $t + (\xi - z)/v_p$ . Hence,

$$\begin{aligned}
 V_2^-(z, t) &= \int_z^l \frac{1}{2} \left( \mathcal{C}_m Z_0 + \frac{\mathcal{L}_m}{Z_0} \right) \frac{\partial}{\partial t} \left[ V_1 \left( t - \frac{\xi}{v_p} - \frac{\xi - z}{v_p} \right) \right] d\xi \\
 &= \frac{1}{2} \left( \mathcal{C}_m Z_0 + \frac{\mathcal{L}_m}{Z_0} \right) \int_z^l \frac{\partial}{\partial t} \left[ V_1 \left( t + \frac{z}{v_p} - \frac{2\xi}{v_p} \right) \right] d\xi \\
 &= -\frac{1}{4} v_p \left( \mathcal{C}_m Z_0 + \frac{\mathcal{L}_m}{Z_0} \right) \int_z^l \frac{\partial}{\partial \xi} \left[ V_1 \left( t + \frac{z}{v_p} - \frac{2\xi}{v_p} \right) \right] d\xi \\
 &= -\frac{1}{4} v_p \left( \mathcal{C}_m Z_0 + \frac{\mathcal{L}_m}{Z_0} \right) \left[ V_1 \left( t + \frac{z}{v_p} - \frac{2\xi}{v_p} \right) \right]_{\xi=z}^l \quad (10.53)
 \end{aligned}$$

or

$$V_2^-(z, t) = K_b \left[ V_1 \left( t - \frac{z}{v_p} \right) - V_1 \left( t - \frac{2l}{v_p} + \frac{z}{v_p} \right) \right] \quad (10.54)$$

where we have defined the *backward-crosstalk coefficient*

$$K_b = \frac{1}{4} v_p \left( \mathcal{C}_m Z_0 + \frac{\mathcal{L}_m}{Z_0} \right) \quad (10.55)$$

Note that the lower limit in the integral in (10.53) is  $z$ , because the line-1 voltage to the left of a given location  $z$  on that line does not contribute to the backward-crosstalk voltage on line 2 at that same location.

For an example to illustrate the application of (10.51) and (10.54), let  $V_g(t)$  in Figure 10.9 be the function shown in Figure 10.12, where  $T_0 < T (= l/v_p)$ . We wish to determine the (+) and (-) wave voltages on line 2.

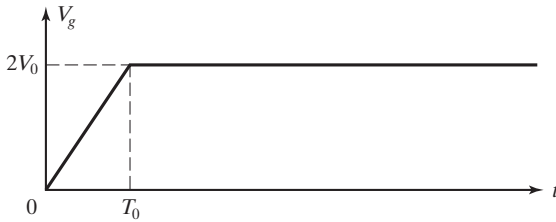


FIGURE 10.12  
Source voltage for the system of  
Figure 10.9.

Noting that

$$V_1(t) = \frac{1}{2} V_g(t) = \begin{cases} (V_0/T_0)t & \text{for } 0 < t < T_0 \\ V_0 & \text{for } t > T_0 \end{cases}$$

and hence

$$V_1'(t) = \begin{cases} V_0/T_0 & \text{for } 0 < t < T_0 \\ 0 & \text{for } t > T_0 \end{cases}$$

and using (10.51), we can write the (+) wave voltage on line 2 as

$$\begin{aligned}
 V_2^+(z, t) &= zK_f V_1'(t - z/v_p) \\
 &= \begin{cases} zK_f V_0/T_0 & \text{for } 0 < (t - z/v_p) < T_0 \\ 0 & \text{otherwise} \end{cases} \\
 &= \begin{cases} zK_f V_0/T_0 & \text{for } (z/v_p) < t < (z/v_p + T_0) \\ 0 & \text{otherwise} \end{cases} \\
 &= \begin{cases} zK_f V_0/T_0 & \text{for } (z/l)T < t < [(z/l)T + T_0] \\ 0 & \text{otherwise} \end{cases}
 \end{aligned}$$

This is shown in the three-dimensional plot of Figure 10.13, in which the cross section in any constant- $z$  plane is a pulse of voltage  $zK_f V_0/T_0$  for  $(z/l)T < t < (z/l)T + T_0$ . Note that the pulse voltage is shown to be negative. This is because normally the effect of inductive coupling dominates that of the capacitive coupling, so that  $K_f$  is negative.

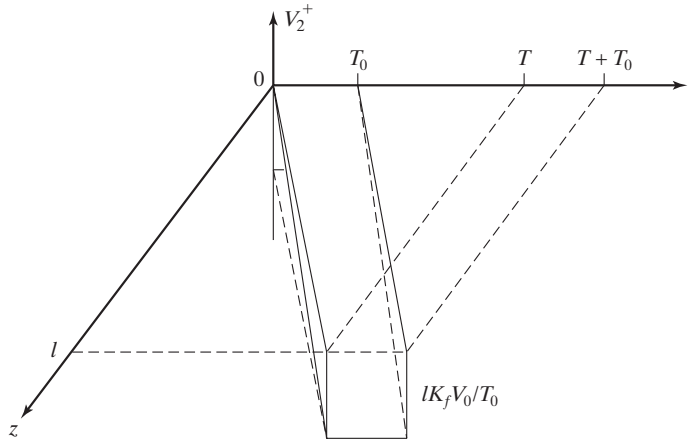


FIGURE 10.13

Three-dimensional depiction of forward-crosstalk voltage for the system of Figure 10.9, with  $V_g(t)$  as in Figure 10.12.

Using (10.54), the (−) wave voltage can be written as

$$V_2^-(z, t) = K_b[V_1(t - z/v_p) - V_1(t - 2l/v_p + z/v_p)]$$

where

$$\begin{aligned}
 V_1\left(t - \frac{z}{v_p}\right) &= \begin{cases} \frac{V_0}{T_0}\left(t - \frac{z}{v_p}\right) & \text{for } 0 < \left(t - \frac{z}{v_p}\right) < T_0 \\ V_0 & \text{for } \left(t - \frac{z}{v_p}\right) > T_0 \end{cases} \\
 &= \begin{cases} \frac{V_0}{T_0}\left(t - \frac{z}{l}T\right) & \text{for } \frac{z}{l}T < t < \left(\frac{z}{l}T + T_0\right) \\ V_0 & \text{for } t > \left(\frac{z}{l}T + T_0\right) \end{cases}
 \end{aligned}$$

$$\begin{aligned}
 V_1\left(t - \frac{2l}{v_p} + \frac{z}{v_p}\right) &= \begin{cases} \frac{V_0}{T_0}\left(t - \frac{2l}{v_p} + \frac{z}{v_p}\right) & \text{for } 0 < \left(t - \frac{2l}{v_p} + \frac{z}{v_p}\right) < T_0 \\ V_0 & \text{for } \left(t - \frac{2l}{v_p} + \frac{z}{v_p}\right) > T_0 \end{cases} \\
 &= \begin{cases} \frac{V_0}{T_0}\left(t - 2T + \frac{z}{l}T\right) & \text{for } \left(2T - \frac{z}{l}T\right) < t < \left(2T - \frac{z}{l}T + T_0\right) \\ V_0 & \text{for } t > \left(2T - \frac{z}{l}T + T_0\right) \end{cases}
 \end{aligned}$$

These two voltages and the  $(-)$  wave voltage for a value of  $z$  for which  $(z/l)T + T_0 < 2T - (z/l)T$  are shown in Figure 10.14. Figure 10.15 shows the three-dimensional plot of  $V_2^-(z, t)$ , in which the cross section in any given constant- $z$  plane gives the time variation of  $V_2^-$  for that value of  $z$ . Note that as  $z$  varies from zero to  $l$ , the shape of  $V_2^-$  changes from a trapezoidal pulse with a height of  $K_b V_0$  at  $z = 0$  to a triangular pulse of height  $K_b V_0$  and width  $2T_0$  at  $z = (1 - T_0/2T)l$  and then changes to a trapezoidal pulse again but with a height continuously decreasing from  $K_b V_0$  to zero at  $z = l$ .

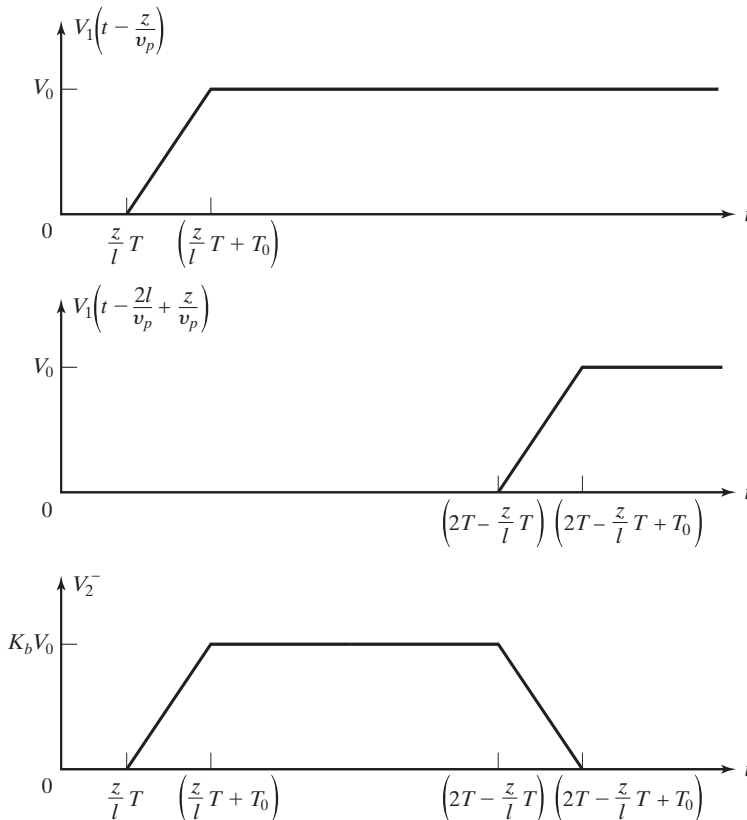


FIGURE 10.14

Determination of backward-crosstalk voltage for the system of Figure 10.9, with  $V_g(t)$  as in Figure 10.12.

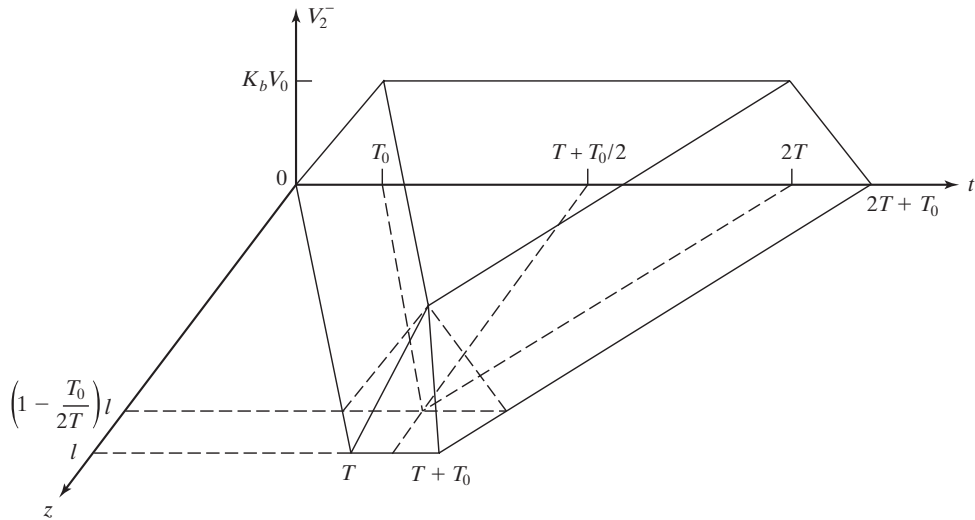


FIGURE 10.15

Three-dimensional depiction of backward-crosstalk voltage for the system of Figure 10.9, with  $V_g(t)$  as in Figure 10.12.

In this section, we studied the topic of crosstalk on transmission lines, by considering the case of weak coupling between two lines. We learned that for a given wave on the primary line, the crosstalk consists of two waves, forward and backward, induced on the secondary line and governed by the forward-crosstalk coefficient and the backward-crosstalk coefficient, respectively. We illustrated by means of an example the determination of crosstalk voltages for a specified excitation for the primary line.

**REVIEW QUESTIONS**

- 10.17. Discuss briefly the weak-coupling analysis for crosstalk between two transmission lines.
- 10.18. Discuss the modeling of capacitive and inductive couplings for crosstalk on transmission lines.
- 10.19. Discuss and distinguish between the dependence of the forward- and backward-crosstalk coefficients on the line parameters.
- 10.20. Outline the determination of the forward- and backward-crosstalk voltages induced on a secondary line for a given excitation for the primary line.

**PROBLEMS**

- 10.11. For the system of Figure 10.9, assume that  $V_g(t)$  is the function shown in Figure 10.16, instead of as in Figure 10.12. Find and sketch the following (a)  $V_2^+(l, t)$ ; (b)  $V_2^-(0, t)$ ; and (c)  $V_2^-(0.8l, t)$ .

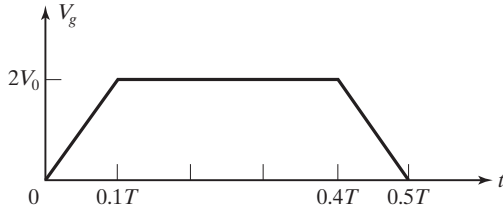


FIGURE 10.16  
For Problem 10.11.

**10.12.** For the system of Figure 10.9, assume that

$$V_g(t) = \begin{cases} 2V_0 \sin^2 \pi t/T & \text{for } 0 < t < T \\ 0 & \text{otherwise} \end{cases}$$

Find and sketch the following: (a)  $V_2^+(l, t)$ ; (b)  $V_2^-(0, t)$ ; (c)  $V_2^-(0.75l, t)$ .

**10.13.** For the system of Figure 10.9, assume that  $K_b/K_f = -25v_p$  and  $T_0 = 0.2T$ . For  $V_g(t)$  given in Figure 10.12, find and sketch the following: (a)  $V_2^+(z, 1.1T)$ ; (b)  $V_2^-(z, 1.1T)$ ; and (c)  $V_2(z, 1.1T)$ .

## 10.5 PARALLEL-PLATE WAVEGUIDE DISCONTINUITY

In Section 8.2, we introduced  $\text{TE}_{m,0}$  waves in a parallel-plate waveguide. Let us now consider reflection and transmission at a dielectric discontinuity in a parallel-plate guide, as shown in Figure 10.17. If a  $\text{TE}_{m,0}$  wave is incident on the junction from section 1, then it will set up a reflected wave into section 1 and a transmitted wave into section 2, provided that mode propagates in that section. The fields corresponding to these incident, reflected, and transmitted waves must satisfy the boundary conditions at the dielectric discontinuity. These boundary conditions were derived in Section 5.5. Denoting the incident, reflected, and transmitted wave fields by the subscripts  $i$ ,  $r$ , and  $t$ , respectively, we have from the continuity of the tangential component of  $\mathbf{E}$  at a dielectric discontinuity,

$$E_{yi} + E_{yr} = E_{yt} \quad \text{at } z = 0 \quad (10.56)$$

and from the continuity of the tangential component of  $\mathbf{H}$  at a dielectric discontinuity,

$$H_{xi} + H_{xr} = H_{xt} \quad \text{at } z = 0 \quad (10.57)$$

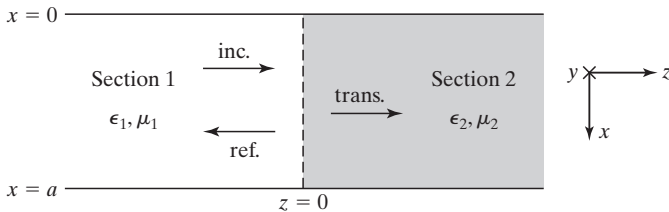


FIGURE 10.17

For consideration of reflection and transmission at a dielectric discontinuity in a parallel-plate waveguide.

We now define the guide characteristic impedance,  $\eta_{g1}$ , of section 1 as

$$\eta_{g1} = \frac{E_{yi}}{-H_{xi}} \quad (10.58)$$

Recognizing that  $\mathbf{a}_y \times (-\mathbf{a}_x) = \mathbf{a}_z$ , we note that  $\eta_{g1}$  is simply the ratio of the transverse components of the electric and magnetic fields of the  $\text{TE}_{m,0}$  wave that give rise

to time-average power flow down the guide. From (8.35a) and (8.35b) applied to section 1, we have

$$\eta_{g1} = \eta_1 \frac{\lambda_{g1}}{\lambda_1} = \frac{\eta_1}{\sqrt{1 - (\lambda_1/\lambda_c)^2}} = \frac{\eta_1}{\sqrt{1 - (f_{c1}/f)^2}} \quad (10.59)$$

The guide characteristic impedance is analogous to the characteristic impedance of a transmission line, if we recognize that  $E_{yi}$  and  $-H_{xi}$  are analogous to  $V^+$  and  $I^+$ , respectively. In terms of the reflected wave fields, it then follows that

$$\eta_{g1} = -\left(\frac{E_{yr}}{-H_{xr}}\right) = \frac{E_{yr}}{H_{xr}} \quad (10.60)$$

This result can also be seen from the fact that for the reflected wave, the power flow is in the negative  $z$ -direction and since  $\mathbf{a}_y \times \mathbf{a}_x = -\mathbf{a}_z$ ,  $\eta_{g1}$  is equal to  $E_{yr}/H_{xr}$ . For the transmitted wave fields, we have

$$\frac{E_{yt}}{-H_{xt}} = \eta_{g2} \quad (10.61)$$

where

$$\eta_{g2} = \eta_2 \frac{\lambda_{g2}}{\lambda_2} = \frac{\eta_2}{\sqrt{1 - (\lambda_2/\lambda_c)^2}} = \frac{\eta_2}{\sqrt{1 - (f_{c2}/f)^2}} \quad (10.62)$$

is the guide characteristic impedance of section 2.

Using (10.58), (10.60), and (10.61), (10.57) can be written as

$$\frac{E_{yi}}{\eta_{g1}} - \frac{E_{yr}}{\eta_{g1}} = \frac{E_{yt}}{\eta_{g2}} \quad (10.63)$$

Solving (10.56) and (10.63), we get

$$E_{yi} \left(1 - \frac{\eta_{g2}}{\eta_{g1}}\right) + E_{yr} \left(1 + \frac{\eta_{g2}}{\eta_{g1}}\right) = 0 \quad (10.64)$$

or the reflection coefficient at the junction is given by

$$\Gamma = \frac{E_{yr}}{E_{yi}} = \frac{\eta_{g2} - \eta_{g1}}{\eta_{g2} + \eta_{g1}} \quad (10.65)$$

and the transmission coefficient at the junction is given by

$$\tau = \frac{E_{yt}}{E_{yi}} = \frac{E_{yi} + E_{yr}}{E_{yi}} = 1 + \Gamma \quad (10.66)$$

These expressions for  $\Gamma$  and  $\tau$  are similar to those obtained in Section 7.2 for reflection and transmission at a transmission-line discontinuity. Hence, insofar as reflection and transmission at the junction are concerned, we can replace the waveguide sections by transmission lines having characteristic impedances equal to the guide characteristic

impedances, as shown in Figure 10.18. It should be noted that unlike the characteristic impedance of a lossless line, which is a constant independent of frequency, the guide characteristic impedance of the lossless waveguide is a function of the frequency.

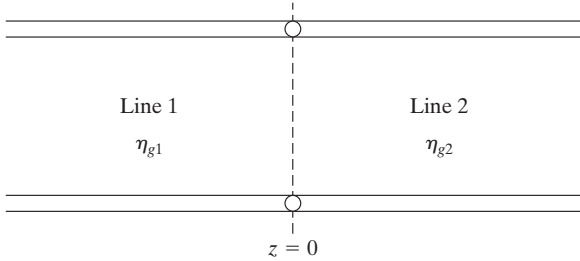


FIGURE 10.18

Transmission-line equivalent of parallel-plate waveguide discontinuity.

For a numerical example of computing  $\Gamma$  and  $\tau$ , let us consider the parallel-plate waveguide discontinuity shown in Figure 10.19, and  $\text{TE}_{1,0}$  waves of frequency  $f = 5000$  MHz, incident on the junction from the free space side.

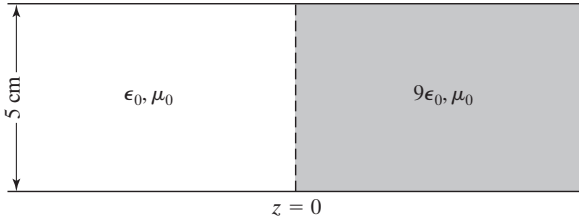


FIGURE 10.19

For illustrating the computation of reflection and transmission coefficients at a parallel-plate waveguide discontinuity.

For the  $\text{TE}_{1,0}$  mode,  $\lambda_c = 2a = 10$  cm, independent of the dielectric. For  $f = 5000$  MHz,

$$\lambda_1 = \text{wavelength on the free space side} = \frac{3 \times 10^8}{5 \times 10^9} = 6 \text{ cm}$$

$$\lambda_2 = \text{wavelength on the dielectric side} = \frac{3 \times 10^8}{\sqrt{9} \times 5 \times 10^9} = \frac{6}{3} = 2 \text{ cm}$$

Since  $\lambda < \lambda_c$  in both sections,  $\text{TE}_{1,0}$  mode propagates in both sections. Thus,

$$\eta_{g1} = \frac{\eta_1}{\sqrt{1 - (\lambda_1/\lambda_c)^2}} = \frac{120\pi}{\sqrt{1 - (6/10)^2}} = 471.24 \Omega$$

$$\eta_{g2} = \frac{\eta_2}{\sqrt{1 - (\lambda_2/\lambda_c)^2}} = \frac{120\pi/\sqrt{9}}{\sqrt{1 - (2/10)^2}} = \frac{40\pi}{\sqrt{1 - 0.04}} = 128.25 \Omega$$

$$\Gamma = \frac{\eta_{g2} - \eta_{g1}}{\eta_{g2} + \eta_{g1}} = \frac{128.25 - 471.24}{128.25 + 471.24} = -0.572$$

$$\tau = 1 + \Gamma = 1 - 0.572 = 0.428$$

For  $f = 4000$  MHz, we would obtain  $\Gamma = -0.629$  and  $\tau = 0.371$ .

In this section, we discussed the solution of problems involving reflection and transmission at a discontinuity in a waveguide by using the transmission-line analogy. This consists of replacing each section of the waveguide by a transmission line whose characteristic impedance is equal to the guide characteristic impedance and then computing the reflection and transmission coefficients as in the transmission-line case. The guide characteristic impedance,  $\eta_g$ , which is the ratio of the transverse electric field to the transverse magnetic field, is given for the TE modes by

$$\eta_g = \frac{\eta}{\sqrt{1 - (\lambda/\lambda_c)^2}} = \frac{\eta}{\sqrt{1 - (f_c/f)^2}} \quad (10.67)$$

## REVIEW QUESTIONS

- 10.21.** Define guide characteristic impedance.
- 10.22.** Provide a physical explanation for why the guide characteristic impedance is different from the intrinsic impedance of the medium in the guide.
- 10.23.** Discuss the use of the transmission-line analogy for solving problems involving reflection and transmission at a waveguide discontinuity.
- 10.24.** Why are the reflection and transmission coefficients for a given mode at a lossless waveguide discontinuity dependent on frequency whereas the reflection and transmission coefficients at the junction of two lossless lines are independent of frequency?

## PROBLEMS

- 10.14.** For the parallel-plate waveguide discontinuity of Figure 10.19, find the reflection and transmission coefficients for  $f = 7500$  MHz propagating in (a)  $TE_{1,0}$  mode and (b)  $TE_{2,0}$  mode.
- 10.15.** The left half of a parallel-plate waveguide of dimension  $a = 4$  cm is filled with a dielectric of  $\epsilon = 4\epsilon_0$  and  $\mu = \mu_0$ . The right half is filled with a dielectric of  $\epsilon = 9\epsilon_0$  and  $\mu = \mu_0$ . For  $TE_{1,0}$  waves of frequency 2500 MHz incident on the discontinuity from the left, find the reflection and transmission coefficients.
- 10.16.** Assume that the permittivity of the dielectric to the right side of the parallel-plate waveguide discontinuity of Figure 10.19 is unknown. If the reflection coefficient for  $TE_{1,0}$  waves of frequency 5000 MHz incident on the junction from the free space side is  $-0.2643$ , find the permittivity of the dielectric.

## 10.6 MAGNETIC VECTOR POTENTIAL AND THE LOOP ANTENNA

In Section 6.1, we learned that since

$$\nabla \times \mathbf{E} = 0$$

for the static electric field,  $\mathbf{E}$  can be expressed as the gradient of a scalar potential in the manner

$$\mathbf{E} = -\nabla V$$

We then proceeded with the discussion of the electric scalar potential and its application for the computation of static electric fields. In this section, we shall introduce a

similar tool for the magnetic field computation, namely, the magnetic vector potential. When extended to the time-varying case, the magnetic vector potential has useful application in the determination of fields due to antennas.

To introduce the magnetic vector potential concept, we recall that the divergence of the magnetic flux density vector, whether static or time-varying, is equal to zero, that is,

$$\nabla \cdot \mathbf{B} = 0 \quad (10.68)$$

If the divergence of a vector is zero, then that vector can be expressed as the curl of another vector, since the divergence of the curl of a vector is identically equal to zero, as can be seen by expansion in Cartesian coordinates:

$$\begin{aligned} \nabla \cdot \nabla \times \mathbf{A} &= \left( \mathbf{a}_x \frac{\partial}{\partial x} + \mathbf{a}_y \frac{\partial}{\partial y} + \mathbf{a}_z \frac{\partial}{\partial z} \right) \cdot \begin{vmatrix} \mathbf{a}_x & \mathbf{a}_y & \mathbf{a}_z \\ \frac{\partial}{\partial x} & \frac{\partial}{\partial y} & \frac{\partial}{\partial z} \\ A_x & A_y & A_z \end{vmatrix} \\ &= \begin{vmatrix} \frac{\partial}{\partial x} & \frac{\partial}{\partial y} & \frac{\partial}{\partial z} \\ \frac{\partial}{\partial x} & \frac{\partial}{\partial y} & \frac{\partial}{\partial z} \\ A_x & A_y & A_z \end{vmatrix} = 0 \end{aligned}$$

Thus, the magnetic field vector  $\mathbf{B}$  can be expressed as the curl of a vector  $\mathbf{A}$ , that is,

$$\mathbf{B} = \nabla \times \mathbf{A} \quad (10.69)$$

The vector  $\mathbf{A}$  is known as the magnetic vector potential in analogy with the electric scalar potential for  $V$ .

If we can now find  $\mathbf{A}$  due to an infinitesimal current element, we can then find  $\mathbf{B}$  for a given current distribution and determine  $\mathbf{B}$  by using (10.69). Let us therefore consider an infinitesimal current element of length  $d\mathbf{l}$  situated at the origin and oriented along the  $z$ -axis, as shown in Figure 10.20. Assuming first that the current is constant

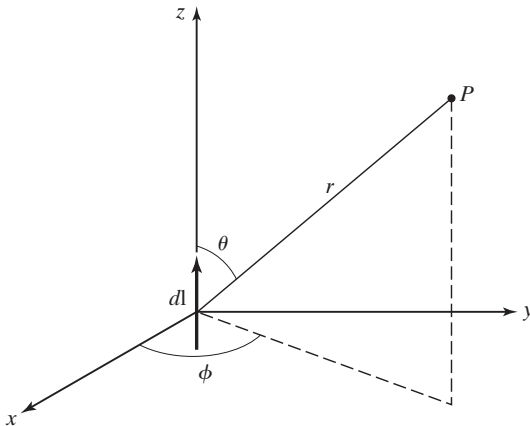


FIGURE 10.20

For finding the magnetic vector potential due to an infinitesimal current element.

and equal to  $I$ , we note from (1.68) that the magnetic field at a point  $P$  due to the current element is given by

$$\mathbf{B} = \frac{\mu}{4\pi} \frac{I d\mathbf{l} \times \mathbf{a}_r}{r^2} \quad (10.70)$$

where  $r$  is the distance from the current element to the point  $P$  and  $\mathbf{a}_r$  is the unit vector directed from the element toward  $P$ . Expressing  $\mathbf{B}$  as

$$\mathbf{B} = \frac{\mu}{4\pi} I d\mathbf{l} \times \left( -\nabla \frac{1}{r} \right) \quad (10.71)$$

and using the vector identity

$$\mathbf{A} \times \nabla V = V \nabla \times \mathbf{A} - \nabla \times (V\mathbf{A}) \quad (10.72)$$

we obtain

$$\mathbf{B} = -\frac{\mu I}{4\pi r} \nabla \times d\mathbf{l} + \nabla \times \left( \frac{\mu I d\mathbf{l}}{4\pi r} \right) \quad (10.73)$$

Since  $d\mathbf{l}$  is a constant,  $\nabla \times d\mathbf{l} = 0$ , and (10.73) reduces to

$$\mathbf{B} = \nabla \times \left( \frac{\mu I d\mathbf{l}}{4\pi r} \right) \quad (10.74)$$

Comparing (10.74) with (10.69), we now see that the vector potential due to the current element situated at the origin is simply given by

$$\mathbf{A} = \frac{\mu I d\mathbf{l}}{4\pi r} \quad (10.75)$$

Thus, it has a magnitude inversely proportional to the radial distance from the element (similar to the inverse distance dependence of the scalar potential due to a point charge) and direction parallel to the element.

If the current in the element is now assumed to be time-varying in the manner

$$I = I_0 \cos \omega t$$

we would intuitively expect that the corresponding magnetic vector potential would also be time-varying in the same manner but with a time-lag factor included, as discussed in Section 9.1 in connection with the determination of the electromagnetic fields due to the time-varying current element (Hertzian dipole). To verify our intuitive expectation, we note from (9.23b) that the magnetic field due to the time-varying current element is given by

$$\begin{aligned} \mathbf{B} &= \mu \mathbf{H} = \frac{\mu I_0 dl \sin \theta}{4\pi} \left[ \frac{\cos(\omega t - \beta r)}{r^2} - \frac{\beta \sin(\omega t - \beta r)}{r} \right] \mathbf{a}_\phi \\ &= \frac{\mu I_0 d\mathbf{l}}{4\pi} \times \left\{ \left[ \frac{\cos(\omega t - \beta r)}{r^2} - \frac{\beta \sin(\omega t - \beta r)}{r} \right] \mathbf{a}_r \right\} \\ &= \frac{\mu I_0 d\mathbf{l}}{4\pi} \times \left\{ -\nabla \left[ \frac{\cos(\omega t - \beta r)}{r} \right] \right\} \end{aligned}$$

and proceed in the same manner as for the constant current case to obtain the vector potential to be

$$\mathbf{A} = \frac{\mu I_0 d\mathbf{l}}{4\pi r} \cos(\omega t - \beta r) \quad (10.76)$$

Comparing (10.76) with (10.75), we find that our intuitive expectation is indeed correct for the vector potential case, unlike the case of the fields in Section 9.1! The result given by (10.76) is familiarly known as the *retarded* vector potential in view of the phase-lag factor  $\beta r$  contained in it.

To illustrate an example of the application of (10.76), we now consider a circular loop antenna having circumference that is small compared to the wavelength so that it is an electrically small antenna. Under this condition, the current flowing in the loop can be assumed to be uniform around the loop. Recall that the electrically small loop antenna as a receiving antenna was introduced in Section 9.6. Let us assume the loop to be in the  $xy$ -plane with its center at the origin, as shown in Figure 10.21, and the loop current to be  $I = I_0 \cos \omega t$  in the  $\phi$  direction. In view of the circular symmetry around the  $z$ -axis, we can consider a point  $P$  in the  $xz$ -plane without loss of generality to find the vector potential. To do this, we divide the loop into a series of infinitesimal elements. Considering one such current element  $d\mathbf{l} = a d\alpha (-\sin \alpha \mathbf{a}_x + \cos \alpha \mathbf{a}_y)$ , as shown in Figure 10.21, and using (10.76), we obtain the vector potential at  $P$  due to that current element to be

$$d\mathbf{A} = \frac{\mu I_0 a d\alpha (-\sin \alpha \mathbf{a}_x + \cos \alpha \mathbf{a}_y)}{4\pi R} \cos(\omega t - \beta R) \quad (10.77)$$

where

$$\begin{aligned} R &= [(r \sin \theta - a \cos \alpha)^2 + (a \sin \alpha)^2 + (r \cos \theta)^2]^{1/2} \\ &= [r^2 + a^2 - 2ar \sin \theta \cos \alpha]^{1/2} \end{aligned} \quad (10.78)$$

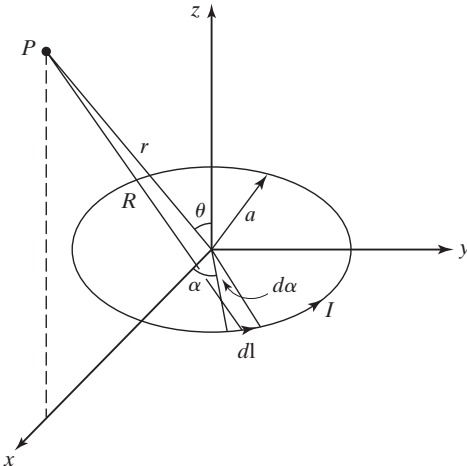


FIGURE 10.21

For finding the magnetic vector potential due to a small circular loop antenna.

The vector potential at point  $P$  due to the entire current loop is then given by

$$\begin{aligned}\mathbf{A} &= \int_{\alpha=0}^{2\pi} d\mathbf{A} \\ &= - \left[ \int_{\alpha=0}^{2\pi} \frac{\mu I_0 a \sin \alpha \, d\alpha}{4\pi R} \cos(\omega t - \beta R) \right] \mathbf{a}_x \\ &\quad + \left[ \int_{\alpha=0}^{2\pi} \frac{\mu I_0 a \cos \alpha \, d\alpha}{4\pi R} \cos(\omega t - \beta R) \right] \mathbf{a}_y\end{aligned}\quad (10.79)$$

The first integral on the right side of (10.79) is, however, zero since the contributions to it due to elements situated symmetrically about the  $xz$ -plane cancel. Replacing  $\mathbf{a}_y$  in the second term by  $\mathbf{a}_\phi$  to generalize the result to an arbitrary point  $P(r, \theta, \phi)$ , we then obtain

$$\mathbf{A} = \left[ \int_{\alpha=0}^{2\pi} \frac{\mu I_0 a \cos \alpha \, d\alpha}{4\pi R} \cos(\omega t - \beta R) \right] \mathbf{a}_\phi \quad (10.80)$$

Although the evaluation of the integral in (10.80) is complicated, some approximations can be made for obtaining the *radiation fields*. For these fields, we can set the quantity  $R$  in the amplitude factor of the integrand equal to  $r$ . For  $R$  in the phase factor of the integrand, we write

$$\begin{aligned}R &= r \left[ 1 + \frac{a^2}{r^2} - \frac{2a}{r} \sin \theta \cos \alpha \right]^{1/2} \\ &\approx r \left[ 1 - \frac{a}{r} \sin \theta \cos \alpha \right]\end{aligned}\quad (10.81)$$

Thus, for the radiation fields,

$$\mathbf{A} = \left[ \int_{\alpha=0}^{2\pi} \frac{\mu I_0 a \cos \alpha \, d\alpha}{4\pi r} \cos(\omega t - \beta r + \beta a \sin \theta \cos \alpha) \right] \mathbf{a}_\phi \quad (10.82)$$

Now, since  $2\pi a \ll \lambda$ , or  $\beta a \ll 1$ , we can write

$$\begin{aligned}\cos(\omega t - \beta r + \beta a \sin \theta \cos \alpha) \\ \approx \cos(\omega t - \beta r) - \beta a \sin \theta \cos \alpha \sin(\omega t - \beta r)\end{aligned}\quad (10.83)$$

Substituting (10.83) into (10.82) and evaluating the integral, we obtain

$$\mathbf{A} = - \frac{\mu I_0 \pi a^2 \beta \sin \theta}{4\pi r} \sin(\omega t - \beta r) \mathbf{a}_\phi \quad (10.84)$$

Having obtained the required magnetic vector potential, we can now determine the radiation fields. Thus from (10.69),

$$\begin{aligned}
 \mathbf{H} &= \frac{\mathbf{B}}{\mu} = \frac{1}{\mu} \nabla \times \mathbf{A} \\
 &= -\frac{1}{\mu r} \frac{\partial}{\partial r} (r A_\phi) \mathbf{a}_\theta \\
 &= -\frac{I_0 \pi a^2 \beta^2 \sin \theta}{4\pi r} \cos(\omega t - \beta r) \mathbf{a}_\theta
 \end{aligned} \tag{10.85}$$

From  $\nabla \times \mathbf{H} = \frac{\partial \mathbf{D}}{\partial t} = \epsilon \frac{\partial \mathbf{E}}{\partial t}$ , we have

$$\begin{aligned}
 \frac{\partial \mathbf{E}}{\partial t} &= \frac{1}{\epsilon} \nabla \times \mathbf{H} = \frac{1}{\epsilon r} \frac{\partial}{\partial r} (r H_\theta) \mathbf{a}_\phi \\
 &= -\frac{I_0 \pi a^2 \beta^3 \sin \theta}{4\pi \epsilon r} \sin(\omega t - \beta r) \mathbf{a}_\phi \\
 \mathbf{E} &= \frac{I_0 \pi a^2 \beta^3 \sin \theta}{4\pi \omega \epsilon r} \cos(\omega t - \beta r) \mathbf{a}_\phi \\
 &= \frac{\eta I_0 \pi a^2 \beta^2 \sin \theta}{4\pi r} \cos(\omega t - \beta r) \mathbf{a}_\phi
 \end{aligned} \tag{10.86}$$

Comparing (10.85) and (10.86) with (9.25a) and (9.25b), respectively, we note that a duality exists between the radiation fields of the small current loop and those of the infinitesimal current element aligned along the axis of the current loop.

Proceeding further, we can find the Poynting vector, the instantaneous radiated power and the time-average radiated power due to the loop antenna by following steps similar to those employed for the Hertzian dipole in Section 9.2. Thus,

$$\begin{aligned}
 \mathbf{P} &= \mathbf{E} \times \mathbf{H} = E_\phi \mathbf{a}_\phi \times H_\theta \mathbf{a}_\theta = -E_\phi H_\theta \mathbf{a}_r \\
 &= \frac{\eta \beta^4 I_0^2 \pi^2 a^4 \sin^2 \theta}{16\pi^2 r^2} \cos^2(\omega t - \beta r) \mathbf{a}_r \\
 P_{\text{rad}} &= \int_{\theta=0}^{\pi} \int_{\phi=0}^{2\pi} \mathbf{P} \cdot \mathbf{r}^2 \sin \theta \, d\theta \, d\phi \, \mathbf{a}_r \\
 &= \int_{\theta=0}^{\pi} \int_{\phi=0}^{2\pi} \frac{\eta \beta^4 I_0^2 \pi^2 a^4 \sin^3 \theta}{16\pi^2} \cos^2(\omega t - \beta r) \, d\theta \, d\phi \\
 &= \frac{\eta \beta^4 I_0^2 \pi^2 a^4}{6\pi} \cos^2(\omega t - \beta r) \\
 \langle P_{\text{rad}} \rangle &= \frac{\eta \beta^4 I_0^2 \pi^2 a^4}{6\pi} \langle \cos^2(\omega t - \beta r) \rangle \\
 &= \frac{1}{2} I_0^2 \left[ \frac{8\pi^5 \eta}{3} \left( \frac{a}{\lambda} \right)^4 \right]
 \end{aligned}$$

We now identify the radiation resistance of the small loop antenna to be

$$R_{\text{rad}} = \frac{8\pi^5\eta}{3}\left(\frac{a}{\lambda}\right)^4 \quad (10.87)$$

For free space,  $\eta = \eta_0 = 120\pi \Omega$ , and

$$R_{\text{rad}} = 320\pi^6\left(\frac{a}{\lambda}\right)^4 = 20\pi^2\left(\frac{2\pi a}{\lambda}\right)^4 \quad (10.88)$$

Comparing this result with the radiation resistance of the Hertzian dipole given by (9.30), we note that the radiation resistance of the small loop antenna is proportional to the fourth power of its electrical size (circumference/wavelength) whereas that of the Hertzian dipole is proportional to the square of its electrical size (length/wavelength). The directivity of the small loop antenna is, however, the same as that of the Hertzian dipole, that is, 1.5, as given by (9.33), in view of the proportionality of the Poynting vectors to  $\sin^2\theta$  in both cases.

In this section, we introduced the magnetic vector potential as a tool for computing the magnetic fields due to current distributions. In particular, we derived the expression for the retarded magnetic vector potential for a Hertzian dipole and illustrated its application by considering the case of a small circular loop antenna. We derived the radiation fields for the loop antenna and compared its characteristics with those of the Hertzian dipole.

## REVIEW QUESTIONS

- 10.25.** Why can the magnetic flux density vector be expressed as the curl of another vector?
- 10.26.** Discuss the analogy between the magnetic vector potential due to an infinitesimal current element and the electric scalar potential due to a point charge.
- 10.27.** What does the word *retarded* in the terminology *retarded magnetic vector potential* refer to? Explain.
- 10.28.** Discuss the application of the magnetic vector potential in the determination of the electromagnetic fields due to an antenna.
- 10.29.** Discuss the duality between the radiation fields of a small circular loop antenna with those of a Hertzian dipole at the center of the loop and aligned with its axis.
- 10.30.** Compare the radiation resistance and directivity of a small circular loop antenna with those of a Hertzian dipole.

## PROBLEMS

- 10.17.** By expansion in Cartesian coordinates, show that

$$\mathbf{A} \times \nabla V = V \nabla \times \mathbf{A} - \nabla \times (V\mathbf{A}).$$

- 10.18.** For the half-wave dipole of Section 9.3, determine the magnetic vector potential for the radiation fields. Verify your result by finding the radiation fields and comparing with the results of Section 9.3.
- 10.19.** A circular loop antenna of radius 1 m in free space carries a uniform current  $10 \cos 4\pi \times 10^6 t$  A. (a) Calculate the amplitude of the electric field intensity at a distance of 10 km in the plane of the loop. (b) Calculate the radiation resistance and the time-average power radiated by the loop.
- 10.20.** Find the length of a Hertzian dipole that would radiate the same time-average power as the loop antenna of Problem 10.19 for the same current and frequency as in Problem 10.19.